Hard Magnetorheological Elastomers: Experimental Characterization, Modeling and Application

Nader Mohseni Ardehali

A Thesis
in
The Department
of
Mechanical, Industrial and Aerospace Engineering

Presented in Partial Fulfillment of the Requirements
For the Degree of Master of Applied Science
Concordia University
Montreal, Quebec, Canada

November 2020

Concordia University

School of Graduate Studies

This is to certify that the thesis prepared

By: **Nader Mohseni Ardehali**

Entitled: **Hard Magnetorheological Elastomers: Experimental Characterization, Modeling and Application**

and submitted in partial fulfillment of the requirements for the degree of

Master of Applied Science

complies with the regulations of this University and meets the accepted standards with respect to originality and quality.

Signed by the final examining committee:

______________________________ Chair

Dr. Behrooz Yousefzadeh

______________________________ Examiner

Dr. Behrooz Yousefzadeh

______________________________ Examiner

Dr. Khaled Galal

______________________________ Thesis Supervisor

Dr. Ramin Sedaghati

Approved ______________________________

Dr. Ivan Contreras, Graduate Program Director

November 17, 2020

____

Mourad Debbabi, Ph.D., Interim Dean
Faculty of Engineering and Computer Science

Abstract

Hard Magnetorheological Elastomers: Experimental Characterization, Modeling and Application

Magnetoactive elastomers also known as Magnetorheological elastomers (MREs) are solid analogue of the well-known magnetorheological (MR) fluids. MREs are smart composite materials made of elastomeric medium embedded with micron-sized ferromagnetic particles. Unlike MR fluids which can mainly provide variable damping, MREs can provide simultaneous variations in damping as well as stiffness properties. Moreover, MREs do not exhibit limitation of MR fluids such as sedimentation of iron particles and leakage. Hard magnetorheological elastomers (H-MREs) are MREs in which the soft magnetic particles in conventional MREs are replaced by hard micron-sized permanent magnetic particles which provide magnetic poles inside the elastomeric medium. By applying the magnetic field in the same or opposite direction of the magnetic poles, respectively, the stiffness of the H-MREs can be increased or decreased. While conventional MREs have been widely studied during the past decade, very limited studies exist to demonstrate the response behavior of H-MREs. The objectives of the present research thesis are to 1- experimentally characterize the viscoelastic properties of H-MREs under varying operating conditions and applied magnetic field, 2- develop simple phenomenological models to predict the viscoelastic response behavior of MREs, 3- explore the potential application of H-MREs in an adaptive vibration isolator. For this purpose, H-MREs with 15% volume fraction of neodymium–iron–boron (NdFeB) magnetic particles have been fabricated and then tested under oscillatory shear motion using a rotational magneto-rheometer to investigate their viscoelastic behavior under varying excitation frequency and magnetic flux density. The influence of the shear strain amplitude and driving frequency are also examined under various levels of applied magnetic field ranging from -0.2 T to 1.0 T. Moreover, field-dependent phenomenological models have been proposed to predict the variation of storage and loss moduli of H-MREs under varying excitation frequency and applied magnetic flux density. The results show that the proposed model can accurately predict the viscoelastic behavior of H-MREs under various fields and operating conditions. Finally, a tunable vibration isolator based on H-MRE is developed and the influence of applying positive and negative magnetic fields on the transmissibility of the HMRE-based isolator is investigated.

Acknowledgments

I would like to express my most veridical gratitude to my supervisor, Prof. Ramin Sedaghati, for his constant encouragement and guidance through all the stages of my study and writing of this thesis. Without his persistent help, the completion of this project would not have been achieved.

I would like to also express my sincere gratitude to Dr. Masoud Hemmatian, for his patience and invaluable guidance and advice throughout my Master's program.

I also wish to acknowledge the great love of my family, my mother, Maryam and my father, Rahim. They supported me unconditionally in all the steps of my life.

I am also greatly indebted to my office-mates and close friends: Hossein Vatandoost, Mostafa Asadi, Armin Rasooli, Fan Lin, Hooman Zoka who have helped me a lot in the past two years.

Table of Contents

List of Figures

List of Tables

Nomenclature

a_B	Field dependent parameters
$a_{B_{0,1,2}}$	Non-dimensional parameter of the model
A	Payload acceleration amplitude
A_g	Ground acceleration amplitude
A_{H-MRE}	Cross- sectional area of H-MRE
b_B	Field dependent parameters
$b_{B_{0,1,2}}$	Non-dimensional parameter of the model
B	Magnetic field intensity
B_m	Magnetic flux density in the H-MRE
c_B	Field dependent parameters
$c_{B_{0,1,2}}$	Non-dimensional parameter of the model
C_{H-MRE}	Equivalent damping of the H-MRE sample
C_c	Critical viscous coefficient
d_B	Field dependent parameters
$d_{B_{0,1,2}}$	Non-dimensional parameter of the model
f	Frequency
F	Force
F_s	Shear force

G	Shear modulus
G_{H-MRE}	Complex shear modulus of the H-MRE
G'	Storage modulus
G'_{Exp}	Storage modulus of experiment
G'_{H-MRE}	Storage modulus of the H-MRE operating in linear viscoelastic region
G'_{Model}	Storage modulus of model
G''	Loss modulus
G''_{Exp}	Loss modulus of experiment
G''_{H-MRE}	Loss modulus of the H-MRE operating in linear viscoelastic region
G''_{Model}	Loss modulus of model
h_{H-MRE}	Thickness of H-MRE specimen
H_m	Magnetic field in MREs
H_s	Magnetic field in the steel
I	Input current
$J_{G'}$	Error function for storage modulus
$J_{G'}$	Error function of the storage modulus
$J_{G''}$	Error function of the loss modulus
K_{H-MRE}	Equivalent stiffness of the H-MRE sample
L	Total length of the flux going through the C-shape steel conduit

$m_{payload}$	Mass of the payload
N	Total turns of coils in the circuit
R^2	Coefficient of determination
T	Transmissibility
x	Displacements of the payload
$\dot{x}$	Velocity of the payload
$\ddot{x}$	Acceleration of the payload
x_g	Displacements of the ground base
λ	Frequency ratio
ξ	Damping ratio
$\emptyset_m$	Magnetic flux in the MRE specimen
ω	Excitation frequency
ω_n	Natural frequency of the isolation system
γ_{lin}	Linear viscoelastic region
γ_s	Shear strain in the H-MRE sample
τ_s	Shear stress in the H-MRE sample

Chapter 1: Introduction, Literature Review and Objectives

Magnetorheological (MR) materials, such as MR fluid, MR foam, MR gel, MR plastomer and MR elastomer are intelligent materials whose rheological and viscoelastic properties can be varied by applying an external magnetic field. The change in their mechanical properties due to the applied magnetic field is fast (less than milli seconds) and is immediately reversible by turning off the magnetic field. MR materials are fabricated by embedding micron-sized magnetizable particles in a non-magnetic matrix such as fluid, gel, or rubber like materials. Research focusing on MR materials was initiated by Jacob Rabinow (Vincent, 1951) through development of magnetorheological fluids (MRFs). MRFs, are colloidal suspensions of micron-sized magnetizable particles in a carrier fluid (such as silicon oil) and exhibit a continuous, rapid and reversible change in the rheological properties, such as viscosity and yield strength, once subjected to an external magnetic field. This behavior is known as the magnetorheological effect or simply MR effect (Rigbi et al., 1983, Lokander et al., 2003b). Upon the application of the magnetic field, the magnetic particles in the free-flowing MR fluid form a chain-like structure along the direction of the applied magnetic field, thus restricting the fluid flow and transforming the MR fluid to a semi-solid condition. Therefore, the force required to break the induced columns of magnetic particles increases with the increase of the applied magnetic field (Carlson et al., 2000) and the corresponding yield stresses enhances. Compared with their electro-rheological (ER) fluid counterparts, MR fluids exhibit an order of magnitude higher yield stress and also less sensitive to the temperature and contaminants (Carlson et al, 2000). MR fluids have been widely used in development of semi-active devices for vibration control applications as these adaptive devices provide reliability and fail-safe feature of the passive systems while maintaining adaptability of fully active systems without requiring large power (Wang et al., 2005, Sodeyama et al., 2004).

Despite their unique features, MR fluids provide only controllable damping and also exhibit some drawbacks such as sedimentation of iron particles and leakage which considerably decrease their control performance over wide operating ranges. MR elastomers (MREs) are solid analogue of MR fluids in which ferromagnetic particles are dispersed into the elastomeric medium (such as natural or silicon rubber). Unlike MR fluids, MREs can provide simultaneous variations on both stiffness and damping properties without issues such as sedimentation of iron particles and leakage (Gong et al., 2005).

1.1 MR Elastomer and its application

Magnetorheological elastomers (MREs) are an emerging class of smart materials that their properties can be changed in a reversible manner under the application of an external magnetic field (Ruddy et al., 2012; Dargahi et al., 2017). The viscoelastic properties of MREs, namely, the storage and loss moduli can be controlled in a rapid, continuous, and reversible manner by applying an external magnetic field (Ginder et al., 1999; Woods et al., 2007). MREs are used in various application such as adaptive tuned vibration absorber (Qian et al., 2017), smart material based isolators (Li et al., 2013), vehicle seat suspension (Du et al., 2011), micro cantilevers (Lee et al., 2014), micro vibrations (Ying et al., 2014), sensors (Wang et al., 2009), touch-screen displays (Chen et al., 2019), magnetometers (Du et al., 2012), prosthetic devices (Jonsdottir et al., 2015), noise barrier systems (Farshad et al., 2004), sandwich beams (Zhou et al., 2005), negative changing stiffness isolators (Sun et al., 2015), bumper of a vehicle (Bogdanov et al., 2009), and particularly in shifting the fundamental frequency of controlled devices.

1.2 Physics of MREs

MREs consist of an elastomeric matrix such as silicon rubber impregnated with micron-sized iron particles and can be classified according to several parameters like particle types, matrix, structure, and distribution of particles. In terms of distribution of particles, MREs can be divided into isotropic and anisotropic MREs (Lu et al., 2012; Asadi Khanouki et al., 2019). Curing the mixture of the elastomer and iron particles in the absence and presence of magnetic field results in isotropic and anisotropic MREs, respectively. In terms of particle types, particles are divided into soft and hard magnetic particles. Soft magnetic particles, such as carbonyl iron (CI) powders, have been widely used in conventional MREs (soft MREs or S-MREs), due to their high saturation magnetization and low remanence (Zhao et al., 2017). Recently, particles of high-coercivity ferromagnetic materials, or hard-magnetic materials, such as neodymium-iron-boron (NdFeB) have also been utilized in soft elastomer matrices to fabricate hard particle based MREs, known as H-MREs. The high remnant characteristics of hard-magnetic materials allow them to retain high residual magnetic flux density even in the absence of magnetic fields once they are magnetically saturated (Wen et al., 2017).

Fabrication of MREs are simple. All required components of MREs should be initially measured for desired weight ratio and then mixed thoroughly. Generally, components are micron-sized ferromagnetic powder (usually CI particles in the case of S-MRE and NdFeB in the case of H-MRE), silicone or natural rubbers, silicone oil and carbon black. Generally, silicone oil is used as an additive in MR elastomer material fabrication. When the molecules of the silicone oil enter the matrix, the space between the matrix molecules are increased, and consequently the conglutination of the molecules is decreased (Li et al., 2013). The fabrication of MREs consisted of three major steps as shown in Figure 1-1: first, the three basic components, micron-sized ferromagnetic powder, the silicone rubber and curing agents, were mixed thoroughly into a homogenous mixture in appropriate proportions. Second, the mixture was put into vacuum chamber for 15 min in order to remove internal air bubbles. Finally, the mixture was placed into a mold and cured at room temperature (25 °C) for one day or in the oven (temperature of around 140 °C to accelerate the curing process) (Fan Lin, 2019).

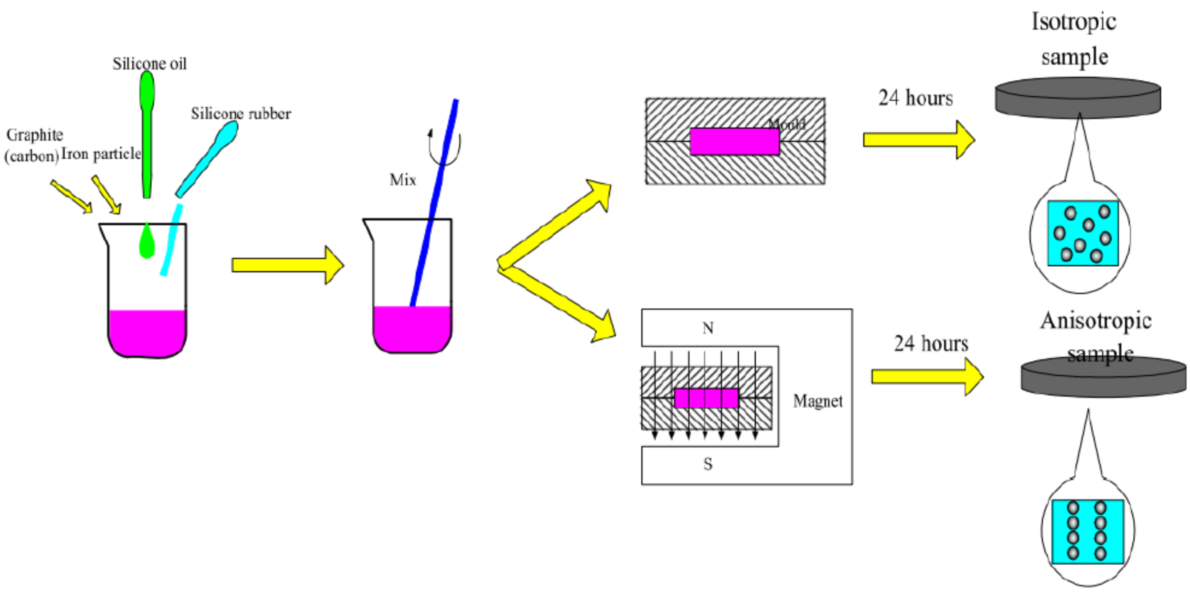

Figure 1-1. Schematic of MRE fabrication process (Megha et al., 2016).

The spatial distribution of the particles is determined during curing process. MREs cured in the absence of the magnetic field would have isotropic structure, as shown in schematic diagrams in Figures 1-1 and 1-2 (A). Presence of a magnetic field during curing results in anisotropic (transversely isotropic) MREs, also known as oriented structure MREs, which consist of chains of particles as schematically shown in Figure 1-1 and 1-2(B). The mechanical properties of MREs depend on many material design factors (such as size and volume fraction of particles, distribution of the particle in the matrix and matrix type), mechanical and magnetic loading (such as excitation strain amplitude and rate, magnitude and direction of the applied magnetic field), as well as environmental conditions (such as temperature) (Chen et al., 2007).

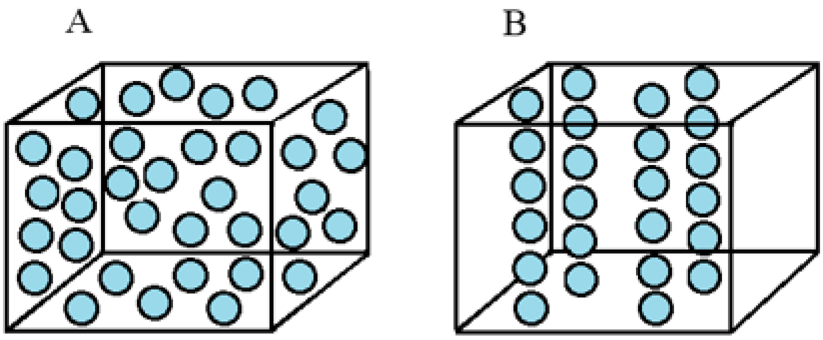

Figure 1-2. Schematic of isotropic (A) and anisotropic (B) MREs.

1.3 Static and dynamic behavior of MREs

Several studies have explored static and dynamic behavior of MREs experimentally. Static properties are generally assessed by measuring the strain-stress or force- displacement characterization of an MRE sample in the presence or absence of an external magnetic field. Dynamic properties are typically evaluated by measuring stress-strain and stress-strain rate responses of the MREs under cyclic motion. The stiffness of MRE is obtained by calculating the major slope of the stress-strain hysteresis curve and the damping is related to the enclosed area inside the hysteresis loop. S-MREs generally behave like a linear viscoelastic material within this linear range which is up to about 10% strain as reported by Dargahi (2017). Li et al., (2013) reported that stress-strain behavior of a large capacity S-MREs (to be used in seismic devices) inclines to be in linear viscoelastic range up to 20% shear strain. Increasing the strain beyond the linear region results in reduction of shear modulus.

In addition to the static and quasi-static properties, dynamic behavior of S-MREs were investigated by scholars to evaluate the influence of magnetic field intensity, driving frequency and strain amplitude on the storage and loss moduli, loss factor and hysteresis properties of S-MREs. In this subject, a typical hysteresis shear stress-shear strain response of an isotropic S-MRE under oscillatory shear motion is shown in Figure 1-3 (Vatandoost et al., 2015). As it can be realized, the slope (representing stiffness) and the enclosed area (representing damping) of hysteresis loops increase with increasing the magnetic flux density. Hysteresis loops are almost elliptical which represent linear viscoelastic behavior of the tested S-MREs up to strain amplitude of 16%. As shown in Figure 1-3(b), S-MREs have shown frequency dependency similar to typical rubbery materials in the linear viscoelastic region and the stiffness and the dissipated energy in MREs increase with increasing the frequency. Deng et al., (2008) also showed that the storage modulus increases approximately linearly by increasing the excitation frequency from 100 Hz to 600 Hz at different magnetic flux ranging from 0 mT to 1000 mT. Lokander et al., (2003) and Kaillo et al., (2007) reported similar trend for the shear modulus. Dargahi et al., (2017) discussed that the dynamic properties of S-MRE with 40% iron particle volume fraction revealed significant hysteresis in stress-strain data and with the application of a 450 mT magnetic flux density, the storage modulus of the S-MRE increases up to 1672% under 2.5% strain amplitude at the frequency of 0.1 Hz, and decreases to nearly 252% under 20% strain amplitude at a frequency of 50 Hz. This large variation in the stiffness of S-MREs confirms their potential to be utilized in adaptive noise and vibration control applications (Dargahi et al., 2017).

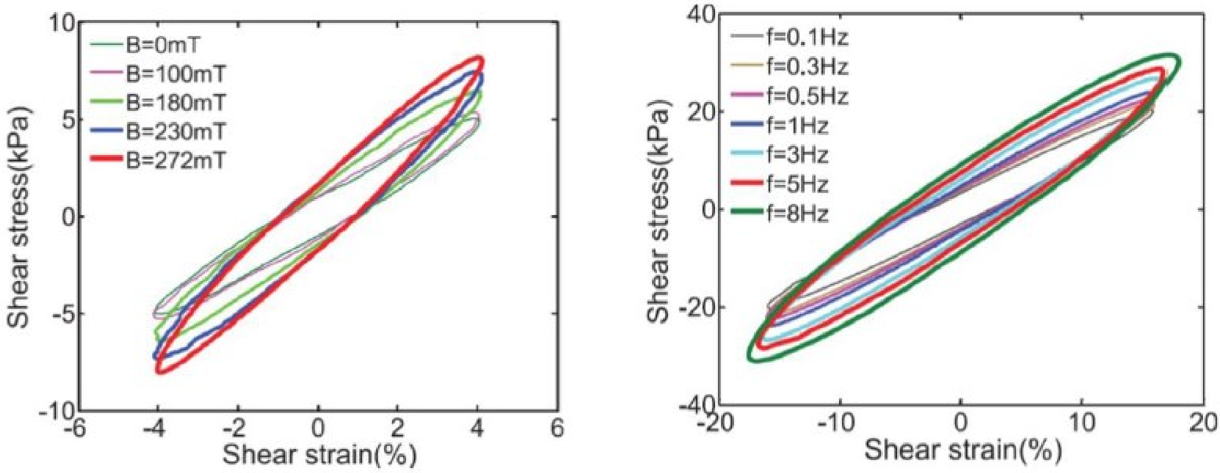

(a) (b)

Figure 1-3. (a): Shear stress-strain behavior of a S-MRE (strain amplitude 4%, and frequency of 0.1 Hz) under different magnetic field intensity; (b) Shear stress-strain behavior of a S-MRE (strain amplitude 16%, magnetic flux density of 272mT) under different excitation frequencies.) (Vatandoost et al., 2015).

One of the main problem with conventional S-MREs is that their storage modulus can be only increased by applying external magnetic field irrespective of the magnetic field direction which limits their potential applications in adaptive MRE based devices such as MRE based vibration absorbers and isolators in which the reduction in the stiffness (or natural frequency) may be required to enhance their control authority. In order to alleviate this issue, an initial magnetic field may be applied either by electromagnet or permanent magnet (Yang et al., 2014) so that the stiffness could be decreased from the initial value by decreasing the applied magnetic field. However, this approach is not effective due to the added cost, weight and power consumption associated with generation of the initial magnetic field (Wen et al., 2017). Thus, hard particle based MREs known as H-MREs, which are capable of providing negative MR effect and reducing their stiffness, seem to be a viable technology to considerably enhance the bandwidth of the MRE based adaptive devices. However, experimental characterization of S-MREs have been widely investigated in the literature, most of reported studies on H-MREs have mainly focused on experimental characterization of H-MREs under limited range of loading conditions such frequency and amplitude. The present research study focuses on H-MREs, thus in the following the pertinent literature with respect to H-MREs has been mainly addressed.

Investigating the actuation capability and viscoelastic properties of H-MREs, Koo et al. (2012) concluded that H-MREs are capable of being used as bending-type actuators. They also measured the block force and tip displacement of the samples to characterize actuation properties of H-MREs. Borin et al. (2013) experimentally determined the tensile modulus of H-MREs and considered the influence of the remanence magnetization on the tensile modulus. The viscoelastic properties of H-MREs also investigated by Stepanov et al. (2012 and 2014) and it was shown that the modulus could be changed in two ways (to increase and decrease) by applying the magnetic field in opposite directions. Moreover, they concluded that the magnetorheological effect of such material is lower than that in magnetically soft composites. Stepanov et al. (2017a) also investigated the mechanism of the re-magnetization of the magnetoactive elastomers with hard magnetic fillers. They explained that this mechanism depends on the re-magnetizing of the magnetic filler and mechanical rotation of particles inside the polymer matrix. Moreover, they investigate the potential of the hybrid magnetic elastomers as active and passive dampers (2017b). Kramarenko et al. (2015) synthesized H-MREs based on a silicone matrix with magnetically hard NdFeB particles and they concluded that the response of H-MRE samples depend on the mutual orientation of the external magnetic field and the internal sample magnetization. Moreover, it was noted that the loss factor increases abruptly when the magnetic field is turned on in the opposite direction to that of sample magnetization due to the particle rotation within the polymer matrix. The loss factor then decreased with time.

Anderson et al. (2015) also reported that anisotropic MREs are stiffer than their isotropic counterparts by examining the dynamic properties of both soft and hard isotropic and anisotropic MREs. The influence of soft and stiff elastomer matrices on the magnetization hysteresis loops of NdFeB based MREs were compared by Kalina et al. (2017) in order to investigate the influence of the matrix material on the rotation of hard magnetic particle. Moreover, they presented microscale model to analyze the macroscopic behavior of H-MREs as a function of the rotation of the embedded particles. In another study conducted by Zhao et al. (2017), the storage modulus of both soft and NdFeB based MR plastomers were analyzed. They demonstrated that unlike soft MR plastomers, the storage modulus of hard MR plastomters kept increasing when the magnetic field decreased and in general the hard MR plastomers presented more complex viscoelastic behavior. Becker et al. (2018) investigated the material properties and vibration of magnetic hybrid elastomer beams fabricated using elastic composite with hard and soft particles aiming to evaluate the potential of magnetic hybrid elastomers to be used in acceleration sensor systems. Hybrid magnetoactive elastomers also have been studied by Borin et al. (2019). They compared the behavior of hybrid magnetoactive elastomers under dynamic axial loading with those of the conventional elastomers. It was shown that both the passive and active state properties of the hybrid magnetoactive elastomer can be tuned using the pre-magnetization of the magnetically hard particles and applied external magnetic field (up to B = 240 mT), respectively.

1.4 Modeling of MREs

Development of predictive models to investigate the dynamic behavior of MREs under various loading conditions is essential to design adaptive MRE-based devices for vibration control applications. Modeling of MRE can be generally divided into four categories, including particle interaction-based, magnetoelastic response-based, magneto-viscoelastic response-based, and phenomenological based models (Cantera et al., 2017).

In the first group of models, particle interaction-based, the focus is mainly dedicated to assess the effect of particle-particle interaction, such as dipole-dipole (Jolly et al., 1996), regular lattice models or chain-like (Asadi et al., 2019). In this category, the present models mainly predict either magneto-induced modulus or stress-strain behavior only in static or quasi-static regime as function of particle size, volume fraction, and particle distribution (Asadi et al., 2019).

Magnetoelastic response-based models predict the coupled magnetic and elastic responses of MREs. These models can be included but not limited to continuum-based models for both small and finite deformation regimes. For instance, Beheshti et al. (2019), developed a continuum-based model by employing linearization technique to construct constitutive equations for predicting magnet-elastic response of isotropic S-MREs subject to small-deformation and finite deformation. These models can be effectively utilized for finite element analysis to design intelligent devices based on MREs with complex geometry subject to different loading condition. However, this category of models cannot see the effect of particle size and mainly predict the coupled behavior in static or quasi-static regime (Cantera et al., 2017).

In the third series, the focus is dedicated to predicting magneto-viscoelastic response of MREs. This approach also includes magneto-viscoelastic continuum-based model (Cantera et al., 2017) and viscoelastic models such as Kelvin-Voigt (Norouzi et al., 2015), and fractional derivative models (Agirre-Olabide et al., 2016) to effectively predict the combination effects of elastic, viscous, and magnetic responses of MREs. However, these models may not be useful to predict highly nonlinear behavior of MREs at large deformation considering wide range of frequency, and also magnetic saturation.

In the last category, the focus is to develop data-driven models based on experimental observations of MREs behavior in response to magnetic and mechanical loadings. For instance, Dargahi et al. (2017) developed a phenomenological model on the basis of a mathematical operator, namely, Prandtle ishlinskii, to capture the behavior of S-MREs as function of loading frequency, and strain amplitude and flux density with four parameters. Unlike the first three groups of models, these types of models can predict the behavior of MREs considering wide range of mechanical (strain and frequency) and magnetic flux density and particularly very useful for design of model-based control strategies.

The vast majorities of reported studies have mainly developed models with different approaches to predict behavior MREs made of magnetically soft particle. However, only a few studies have assessed the behavior of MRE made of magnetically hard particles which are limited to specific loading conditions. For instance, Wen et al. (2017) developed a quasi-static dipolar model to explain mechanical behavior of H-MRE under external magnetic fields subject to only frequency of 5 Hz.

While there are a number of studies on H-MREs and their quasi-static modeling using the microscale approach, no study have been reported on characterization of H-MREs under wide range of operating conditions, particularly investigation on the effect of excitation frequency and negative magnetic field.

1.5 Adaptive Vibration Isolator

Vibration is the major cause of structural fatigue failure. Moreover, long term exposure to excessive vibration can cause severe adverse health effect. In order to mitigate the excessive vibration, MRE-based isolators/absorbers have become promising adaptive devices to mitigate vibration semi-actively over a wide frequency range. This is mainly due to the fact that the modulus of MRE can be controlled rapidly, continuously, and reversibly by an external magnetic field. These MRE-based devices possess fail-safe and reliability of the passive systems while maintaining adaptability of the fully active devices without having large power requirement and complex control hardware. Many studies reported the applications of MREs to adaptive tuned vibration absorbers. Ginder et al. (2001) investigated the development of an adaptive tunable vibration absorber using S-MREs. Deng et al. (2006) used S-MREs to design a tunable vibration absorber with a frequency range of 55–82 Hz. Lerner and Cunefare (2008) developed three vibration absorber configurations with S-MREs in shear, longitudinal, and squeeze modes, respectively. Ni et al. (2009) proposed a dynamic stiffness-tuning absorber with squeeze-strain-enhanced S-MREs. Ginder et al. (2000) exploited S-MREs to construct a proof-of-concept mounting and isolation in automotive. Hitchcock et al. (2006) proposed a device based on S-MREs to control the response of a structure to shock events. Opie and Yim (2009) explored a tunable stiffness MRE vibration isolator, and by comparing to passive systems they concluded that MRE isolator with semi-active controller system reduced resonances and payload velocities by 16%–30%. Real-time tunable vibration isolators are more advantageous than the passive isolators, such as metal rubber isolator, as the isolators' natural frequency can be adaptively changed to accommodate unpredicted environmental conditions (Liao et al., 2015). While soft MREs (S-MREs) having widely used in development of MRE-based devices, studied on application of hard MREs (H-MREs) in adaptive isolators are very limited. In this study, the vibration isolation performance of a tunable vibration isolator based on H-MRE under varying applied current has been investigated by modeling the H-MRE based isolator as a single-degree-of-freedom system.

1.6 Scope and objectives

The overall goal of this dissertation is to fabricate and characterize the behavior of H-MREs under oscillatory shear mode to investigate their viscoelastic properties under varying excitation frequency and magnetic flux density. Moreover, this study aims at development of a simple phenomenological model to investigate the dynamic behavior of H-MRE under different loading conditions. The specific objectives of the study are as follows:

1. Fabrication and characterization of the dynamic magneto-mechanical properties of H-MREs under wide ranges of loading conditions and applied magnetic field intensities;

2. Developing a phenomenological based mathematical model to predict the dynamic behavior of the H-MRE over wide ranges of loading frequencies and magnetic field intensities.

3. Investigating the vibration isolation performance of a tunable vibration isolator based on H-MRE under both positive and negative magnetic fields.

1.7 Organization of the dissertation

This dissertation is organized into five chapters. First chapter includes some introductory topics on MREs and their fabrication and characterization procedure as well as a pertinent literature review with focus on H-MREs. Chapter 2 describes the experimental characterization of H-MREs, including the fabrication of the isotropic H-MRE samples, test setup and characterization of the H-MRE followed by investigating the effect of different loading conditions and applied magnetic field on viscoelastic properties. Chapter 3 provides details on the modeling of H-MREs. In this chapter a field- and frequency-dependent phenomenological model is proposed to predict the variation of storage and loss moduli of H-MREs as function of the excitation frequency and applied magnetic flux density. A tunable vibration isolator based on H-MRE is developed in Chapter 4 and the transmissibility of the system under the both positive and negative magnetic field is investigated. Finally, chapter 5 provides conclusion and summary of contributions together with some remarks for future studies.

Chapter 2: Fabrication and Characterization of H-MREs

2.1 Introduction

In this chapter, first the procedure of fabricating the isotropic H-MRE samples is explained. This is then followed by the description of the experimental test setup and experimental tests that have been conducted to characterize the viscoelastic properties of H-MREs. Then, the obtained data were analyzed in order to investigate the effect of different loading conditions including of the shear strain amplitude, excitation frequency and magnetic flux density on the storage and loss moduli of H-MREs. To effectively exploit H-MREs in the design of H-MRE-based adaptive devices or structures, it is of paramount importance to fundamentally investigate and characterize their dynamic behavior in wider range of frequency and excitation amplitudes. While there are a number of studies on dynamic characterization of H-MREs, they are mostly limited to limited range of frequency and amplitude of excitation. Considering this, the dynamic behavior of H-MREs operating in oscillatory shear mode are investigated in the wide range of frequency, strain amplitude and magnetic flux density.

2.2 Experimental Characterization of H-MREs

2.2.1 Fabrication of isotropic H-MRE samples

The H-MRE samples with 15% volume fraction of hard magnetic particles were fabricated in the laboratory by mixing hard magnetic particles and silicone rubber matrix. The hard magnetic particles were unmagnetized NdFeB particles with a mean particles size of approximately 50 μm and the silicone rubber (Ecoflex 00-50; Smooth On) was used as the matrix of H-MRE. First, the NdFeB particles and the silicone rubber were mixed thoroughly for about 5 min. to obtain a homogenous mixture. The mixture was then degassed in a vacuum chamber under -28 in-Hg for about 5 min. Afterward, the mixture was poured into a transparent plexi-glass mold and left for 24 hours at room temperature to be cured. Finally, the cured material was cut into 20 mm diameter cylindrical samples. The samples were then magnetized using a double-yoke adjustable electromagnet under 2.7 T magnetic flux density with applied magnetic field along the axis of the cylindrical samples. The distance between the yokes is set according to the total thickness of H-MRE specimen (2 mm). Figure 2-1 shows the microstructure image of the H-MRE with two different scale. It is noted that the fabricated H-MRE samples are isotropic and no external magnetic field has been applied to the samples during the curing process. Therefore the hard particles (white spots in microstructure images) were distributed randomly inside the elastomer matrix.

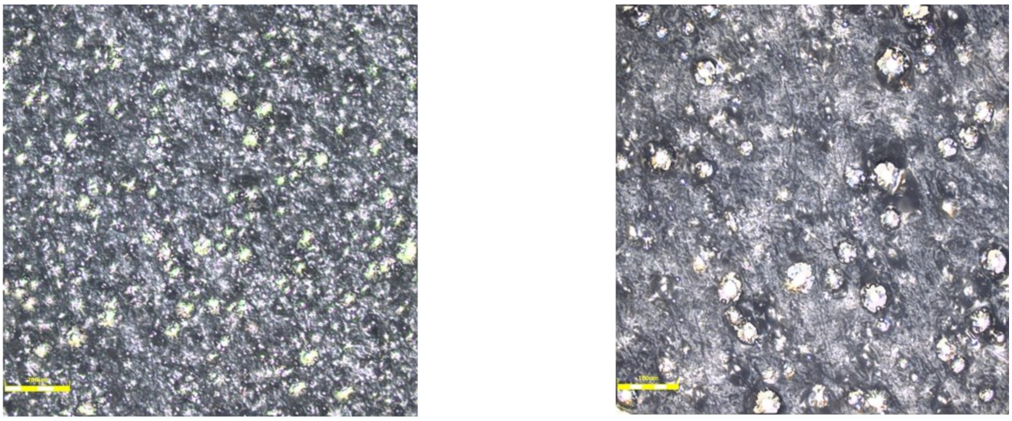

(a) (b)

Figure 2-1. Microstructure images of fabricated H-MRE sample taken by Confocal microscopy; (a) Scale = 200 µm (10x zoom) and (b) Scale = 100 µm (20x zoom).

2.2.2 Test setup

The viscoelastic properties of the H-MRE samples were measured using an advanced rotary rheometer (Discovery HR-3, TA instrument) equipped with magnetorheology accessory as shown in Figure 2.2. The accessory is capable of applying uniform magnetic field ranging from -1.0 T to 1.0 T along the central axis, perpendicular to the circular cross-section, of the H-MRE sample while keeping the temperature uniform and constant. In the present study, the applied magnetic field is addressed as positive or negative when it is in the same or opposite direction compared to the direction of the magnetic poles inside the H-MRE sample, respectively. The test sample (20 mm diameter and 2 mm thickness) was placed between the rotating and fixed parallel geometries. The sample was initially subjected to 30 N axial compression load during all the tests in order to ensure that there is no slippage between the geometries and the sample. For this purpose, 30 N axial load was applied before starting each test and then the gap between the upper and lower plates was maintained constant during the oscillatory shear tests. In other words, the tests have been done under constant pre-strain corresponding to 30 N axial load. Applying magnetic field increases the stiffness of the sample and therefore the measured axial load increases when the magnetic field is applied. The increase in the axial load could also be due to the magnetostrictive property of H-MREs which causes the sample to elongate in presence of magnetic field. It should be mentioned that the axial load goes back to 30 N upon removal of the magnetic field. The temperature of the sample was kept constant during the tests at 20 ℃ by circulating cooling fluid through the magnetorheology accessory.

Figure 2-2. Discovery HR-3, TA instrument.

2.2.3 Design of experiments

The viscoelastic properties of H-MREs depend on the operating conditions including the amplitude and frequency of excitation and applied magnetic flux density. In the present study, two sets of experiments were designed in order to investigate the dynamic viscoelastic behavior of H-MREs operating in different loading conditions. First, the storage and loss moduli of the H-MRE sample were evaluated by sweeping the shear strain amplitude between 0.01% to 5%, while the driving frequency was kept steady. The tests were conducted under different levels of applied magnetic flux density. The purpose of this test was to identify the linear viscoelastic region in which the storage and loss moduli are independent of the strain amplitude. Then, the influence of the excitation frequency on the storage and loss moduli of the H-MRE was investigated through sweep frequency tests. For this purpose, the oscillatory shear tests were performed at linear shear strain amplitude of 0.01% while the excitation frequency was swept from 0.1 Hz to 60 Hz. It should be noted that all the tests have been performed under both positive and negative applied magnetic flux densities and the effect of negative magnetic field on the storage and loss moduli of the H-MRE samples were evaluated.

2.3 Experimental Results and Discussion

The obtained experimental data were subsequently analyzed to investigate the effect of different loading conditions on the viscoelastic properties of H-MREs. These have been addressed in the following sections.

2.3.1 Effect of shear strain amplitude

In order to investigate the influence of shear strain amplitude on the storage and loss moduli of H-MRE's, the oscillatory shear tests were performed by sweeping the strain amplitude in the range of 0.01% to 5% under 1, 5, 10, and 20 Hz driving frequencies, while the temperature maintained steady at 20 °C. The tests were implemented under various levels of positive and negative applied magnetic flux densities varied from B = -0.2 T to B=1 T to also study the effect of applied magnetic field on the mechanical properties of the H-MRE. The variation of the storage modulus with respect to the shear strain amplitude under different magnetic field densities at excitation frequency of 1 Hz are shown in Figure 2-3. As it can be realized, the storage modulus is independent of strain amplitude for excitations with strain amplitudes below 0.1 %. The storage modulus decreases by further increase of the strain amplitude demonstrating the nonlinear viscoelastic behavior of H-MRE. The strain softening effect can be explained by the breakdown of filler aggregates leading to release trapped rubber for allowing more viscous flow, disconnection of dipole-dipole interaction between neighbor particles and filler rubber detachment and reformation that is intensified by increasing the strain amplitude (Rendek et al., 2010, Dargahi., 2017). The region in which the storage modulus is independent of the strain amplitude is called linear viscoelastic region and the associated strain amplitude is represented as $\gamma_{lin.}$. Figure 2.3 also demonstrates that the storage modulus increases by increasing the applied magnetic flux density. It is noted that the rate of increase in the storage modulus decreases as the magnetic field increases due to the magnetic saturation. Moreover, unlike the S-MREs, applying magnetic field in the direction opposite to the orientation of the magnetization weakens the magnetic bonding between the hard particles and consequently reduces the storage modulus of the H-MRE. Thus, it is possible to make the H-MRE softer or stiffer by changing the direction of magnetic field. This behavior significantly increases the control effectiveness of H-MRE-based devices and offers a unique opportunity to utilize H-MREs in different vibration control applications in which both negative and positive variation of the stiffness is required.

Figure 2-4 shows the variation of the loss modulus with respect to the strain amplitude at excitation frequency of 1 Hz under different applied magnetic flux densities. Results show that the loss modulus is generally less sensitive to strain amplitude compared with the storage modulus. Figure 2-4 also shows that regardless of the orientation of the magnetization, applying magnetic field causes the loss modulus of the H-MRE to increase. Increasing the applied magnetic field in positive direction increases the loss modulus, however, this increment is very slight compared with that of storage modulus. On the other hand, the effect of negative field on the loss modulus is in contrary with that on the storage modulus as presented in Figure 2-3. This is mainly due to the fact that applying negative magnetic field causes the magnetized particles to rotate in the matrix which enhances the energy dissipation capacity of the H-MRE and, subsequently its loss modulus. Moreover, it is clear in Figure 2-4 that the loss modulus is almost strain-independent for the strain amplitude range of 0.01% to almost 5% regardless of the applied magnetic flux density.

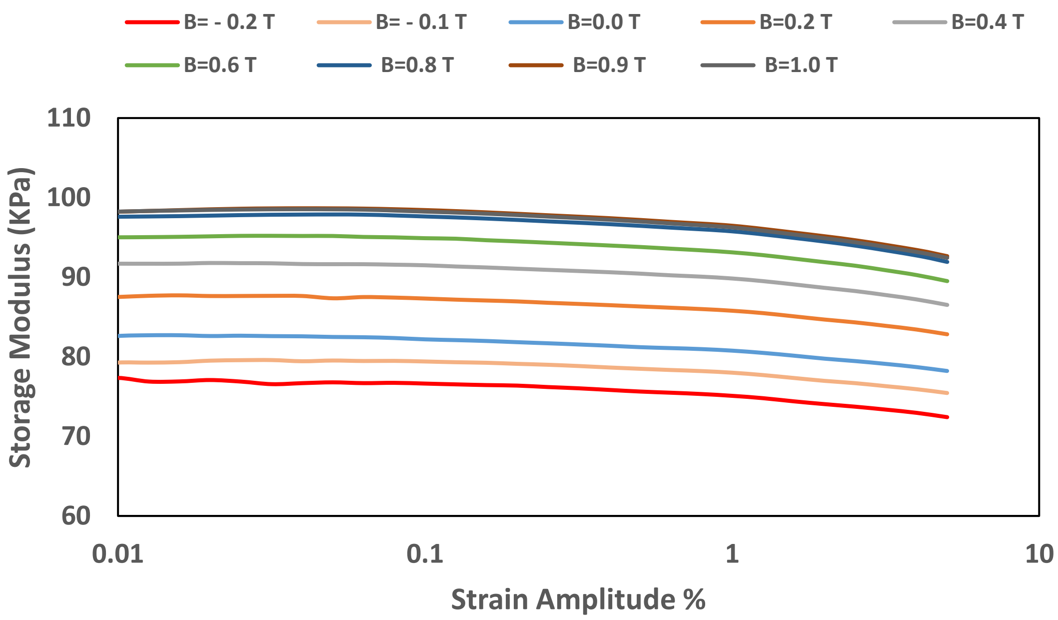

Figure 2-3. Variation of storage modulus with respect to the shear strain amplitude at the excitation frequency of 1 Hz for various applied magnetic flux densities.

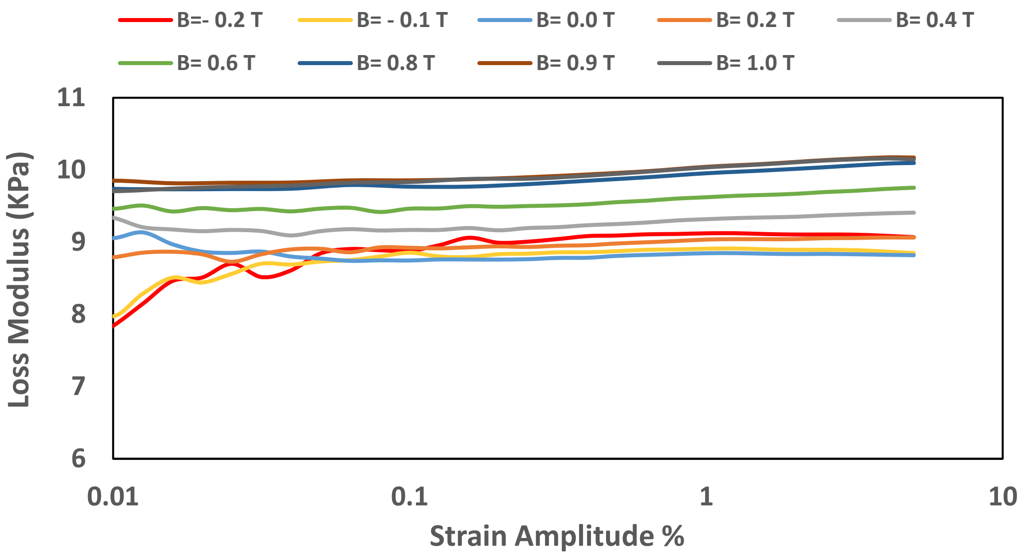

Figure 2-4. Variation of loss modulus with respect to the shear strain amplitude at the frequency of 1 Hz for various applied magnetic flux densities.

Results for variation of storage and loss module with respect to strain amplitude at excitation frequencies 5, 10, and 20 Hz are also shown in Figure 2-5 to Figure 2-10. As it can be realized, similar trend can be observed at higher excitation frequencies. For instance, the storage modulus is independent of strain amplitude for strain amplitudes below 0.1 % and further increase of the strain amplitude decreases the modulus demonstrating the nonlinear viscoelastic behavior. Moreover, it can be observed that the strain-softening effect is more pronounced under higher magnetic field intensities. This is mainly due the fact that increasing the strain will lead to increase in the distance between the dipoles and at a certain distance, the magnetic network that was structured by the dipoles will break down causing a significant decrease in shear modulus of MRE. It is noted that that strain-softening effect is also referred to Flether-Gent effect (Fletcher.,1954) also known as Payne effect (Payne et al., 1971). This phenomenon is defined as the decrease of shear storage modulus with increasing amplitude of oscillation (Leblanc., 2002, Payne et al., 1971). At the specific applied magnetic field by increasing the strain, the magnetic force between magnetic particles, which are embedded in the matrix, becomes less. Hence, the shear modulus of MRE is decreased by increasing the strain amplitude as shown in experimental results. In other words, the MRE shows strain-softening behavior.

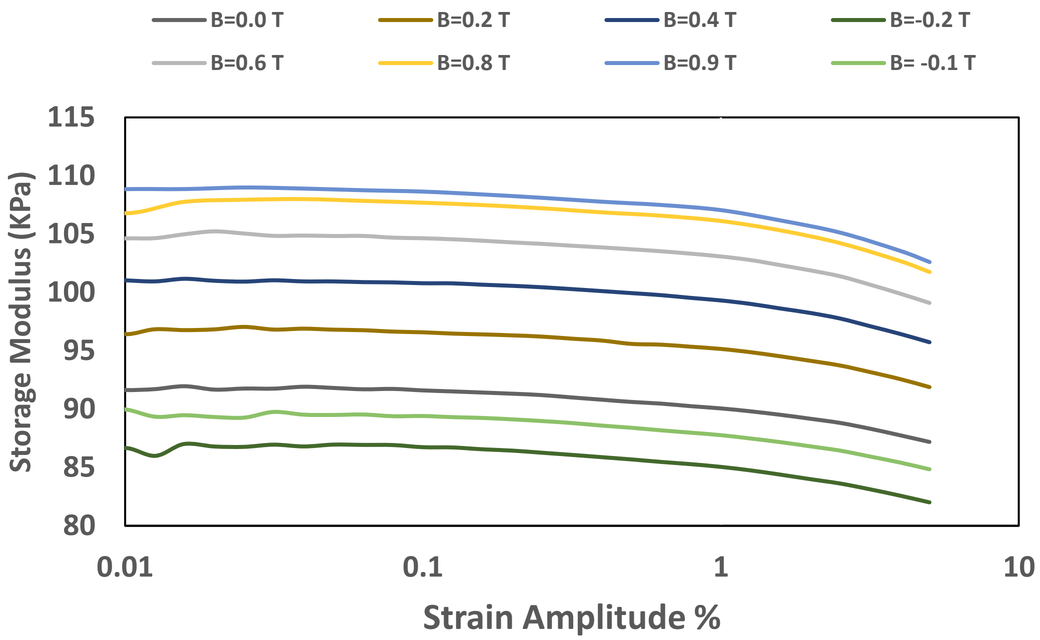

Figure 2-5. Variation of storage modulus with respect to the shear strain amplitude at the excitation frequency of 5 Hz for various applied magnetic flux densities.

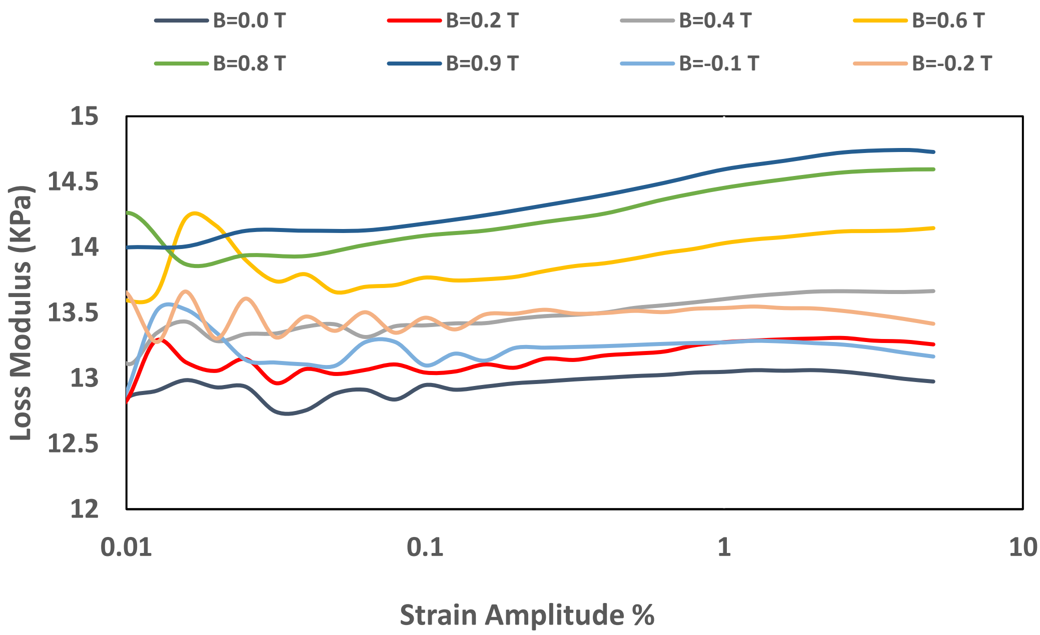

Figure 2-6. Variation of loss modulus with respect to the shear strain amplitude at the frequency of 5 Hz for various applied magnetic flux densities.

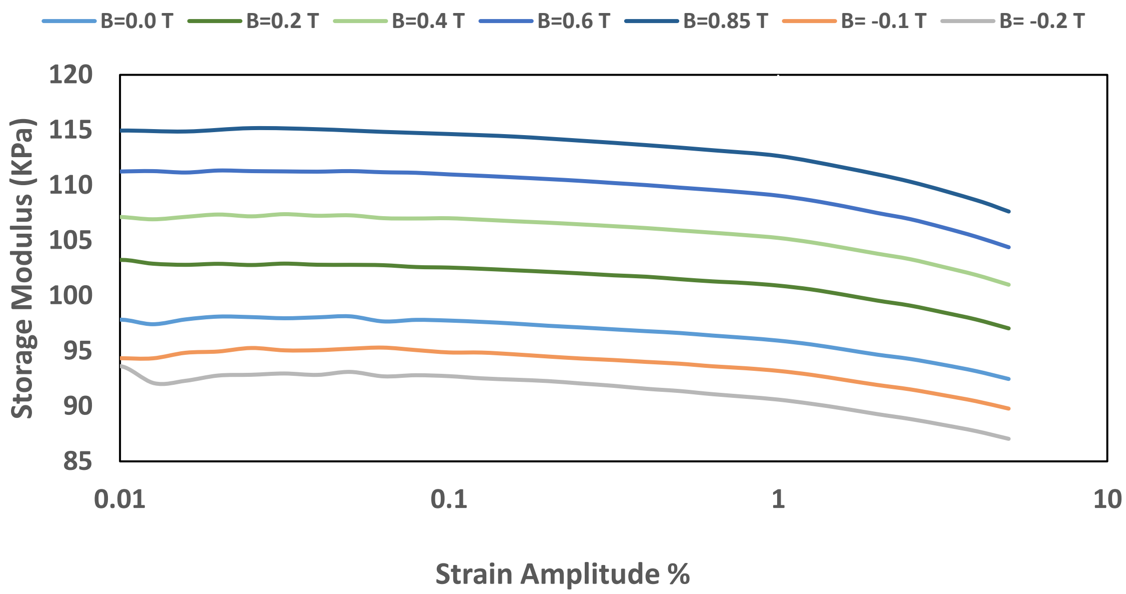

Figure 2-7. Variation of storage modulus with respect to the shear strain amplitude at the excitation frequency of 10 Hz for various applied magnetic flux densities.

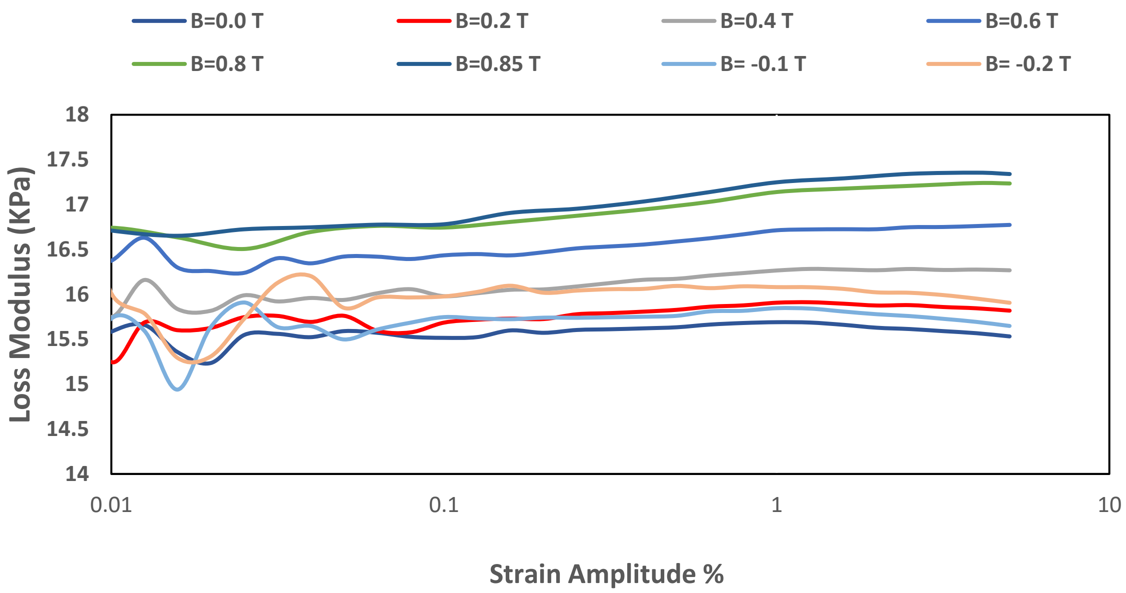

Figure 2-8. Variation of loss modulus with respect to the shear strain amplitude at the frequency of 10 Hz for various applied magnetic flux densities.

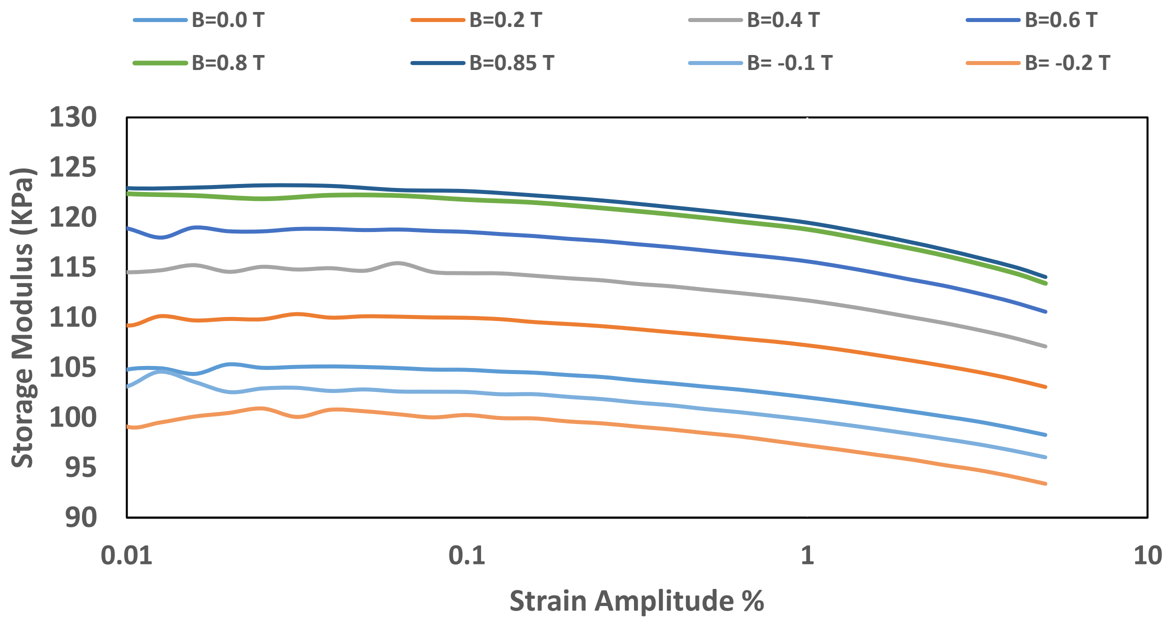

Figure 2-9. Variation of storage modulus with respect to the shear strain amplitude at the excitation frequency of 20 Hz for various applied magnetic flux densities.

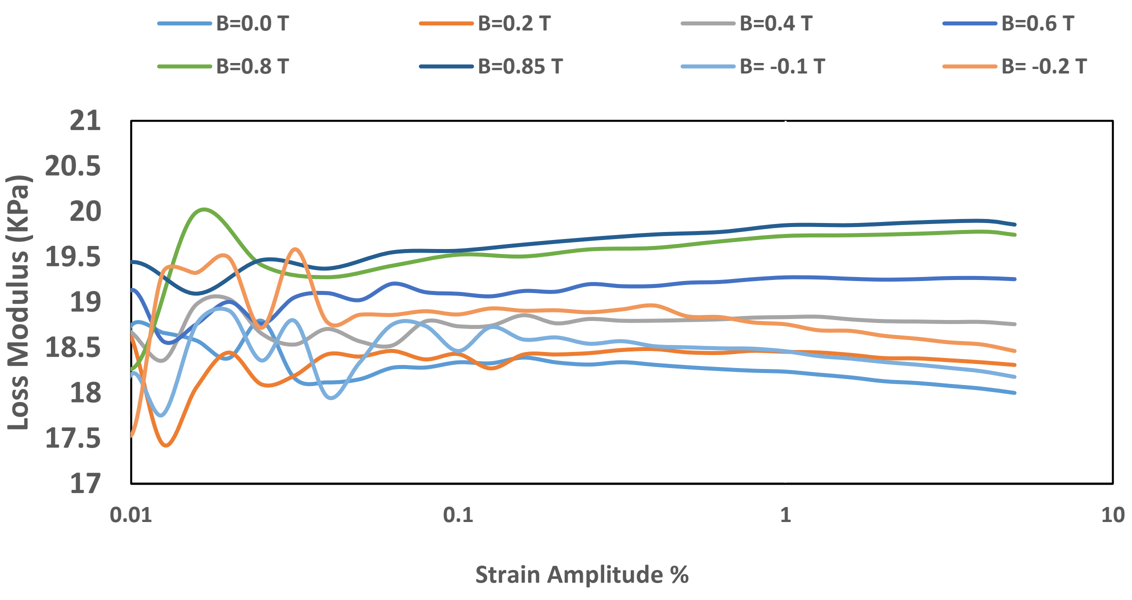

Figure 2-10. Variation of loss modulus with respect to the shear strain amplitude at the frequency of 20 Hz for various applied magnetic flux densities.

2.3.2 Effect of excitation frequency

Sweep frequency tests have been performed in order to investigate the effect of excitation frequency on the behavior of H-MREs operating in shear mode. For this purpose, the oscillatory shear tests were conducted under constant shear strain amplitude of 0.01% (linear region), while the frequency was swept in the range of 0.1 to 60 Hz. The tests were performed under various magnitudes of applied magnetic flux densities ranging from -0.2 T to B=0.85 T in order to investigate the effect of both negative and positive magnetic field on the dynamic behavior of H-MREs. Figures 2-11 and 2-12 show the variation of the storage and loss moduli with respect to the excitation frequency for different levels of applied magnetic flux densities. Results presented in Figure 2-11 show that the storage modulus increases by increasing driving frequency (rate stiffening effect). Results show that the storage modulus increases almost exponentially at low frequencies between 0.1 to 10 Hz (region (a)) while the rate of increase in storage modulus reduces noticeably in this region. Further examination of results reveals that the rate of increase in storage modulus becomes constant and the modulus increases almost linearly beyond 10 Hz (region (b)), thus one may assume linear variation of the storage modulus with respect to the excitation frequency in this region. This behavior could be due to the fact that by increasing the driving frequency, the measurement duration becomes less than the lifetime of the bonding between the matrix chains as well as the silicone rubber matrix and hard magnetic particles. Therefore, the effective bonding increases at higher frequencies which contributes to higher storage modulus of the H-MRE. In addition, Figure 2-11 shows that apart from the driving frequency, the storage modulus increases by increasing the magnetic flux density and the trend of increment is quite similar over the observed frequency range.

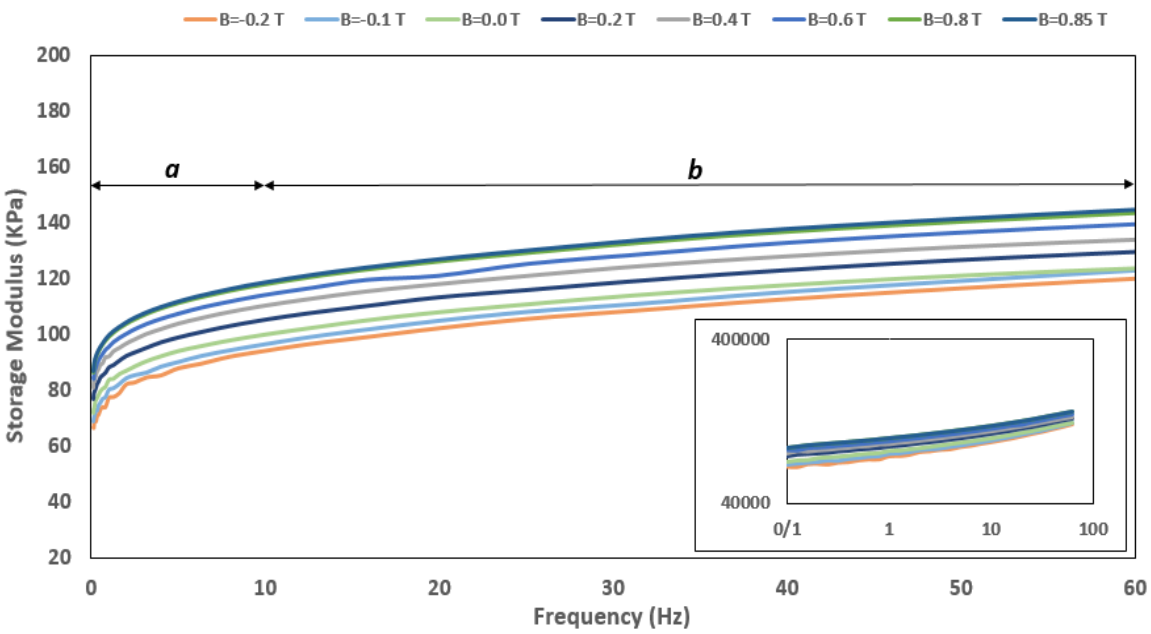

Figure 2-11. Storage modulus with respect to the driving frequency for different applied magnetic flux densities in both linear and logarithmic scales.

Figure 2-12 shows the variation of the loss modulus versus frequency for different magnetic flux densities. Increasing the excitation frequency rises the intermolecular heat generated inside the H-MRE sample and consequently the energy dissipation in the H-MRE increases by increasing the excitation frequency. This phenomenon appears as the growth in the loss modulus with respect to the frequency. As shown in Figure 2-12, the trend of variation in loss modulus with respect to the driving frequency is similar to that of the storage modulus. The loss modulus increases almost linearly in frequencies higher than 10 Hz (region b), whereas, the loss modulus increases almost exponentially for frequencies lower than 10 Hz (region (a)). With respect to the influence of the applied magnetic flux density, as discussed before unlike the storage modulus, applying magnetic field in the opposite direction as the direction of the magnetization does not reduce the loss modulus. Results show that the level of the loss modulus is almost the same for -0.2 T and 0.2 T applied magnetic flux densities. For instance, for 60 Hz excitation frequency, the loss modulus is 23.68 KPa and 23.2KPa in presence of -0.2 T and 0.2 T applied magnetic flux densities, respectively. Moreover, the influence of the applied magnetic field on the loss modulus is not significant compared with its effect on the storage modulus and only applying significant amount of magnetic field (e.g. 0.85 T) causes a slight enhancement in the loss modulus.

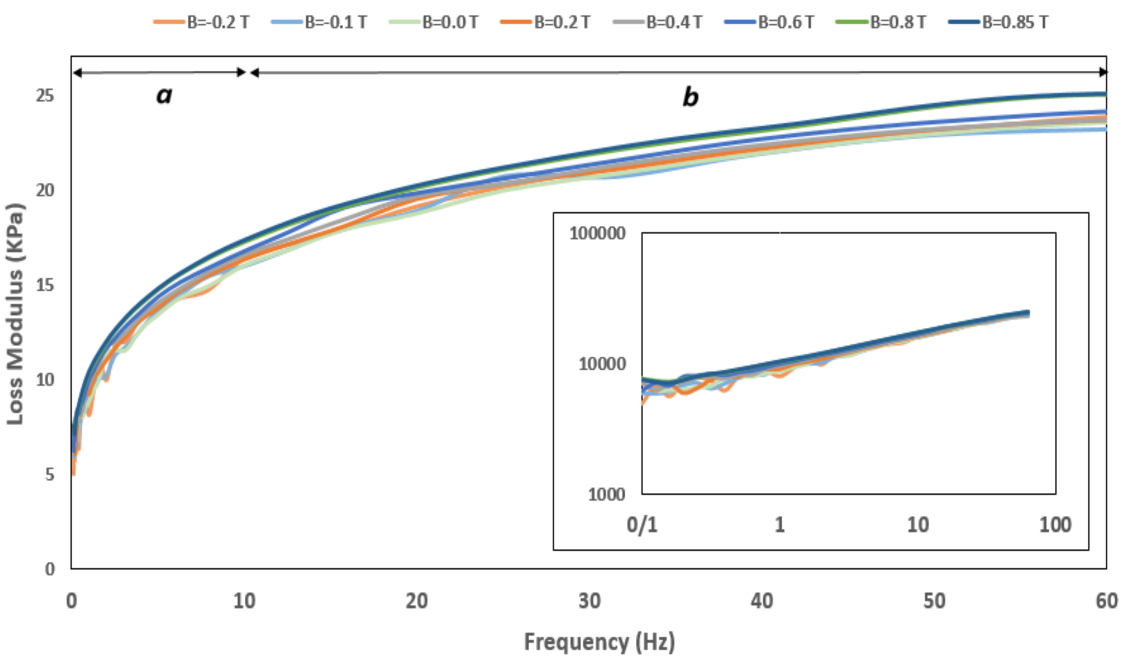

Figure 2-12. Loss modulus with respect to the driving frequency for different applied magnetic flux densities in both linear and logarithmic scales.

2.3.3 Effect of applied magnetic field

Magnetic field intensity is the major factor that affects the dynamic behavior of MREs. Variation of the storage modulus of the H-MRE with respect to the applied magnetic flux density, for different driving frequencies, are shown in Figures 2-13, 2-14 and 2-15. Results are generated at various levels of shear strain amplitudes ranging from 0.01% to 5% at driving frequency ranging from 1 Hz 10 Hz. Results clearly show that the storage modulus increases with an increase of the applied magnetic flux density up to saturation limit of almost 0.8 T after which further enhancement of the field does not noticeably affect the modulus. This can be attributed to the magnetic saturation of the particles above 0.8 T. This behavior was observed at all excitation frequencies and strain amplitudes. The enhancement of the storage modulus demonstrates field stiffening effect of H-MREs which could potentially utilized for vibration control applications. Moreover, results again clearly confirm that storage modulus reduces by applying magnetic field in the opposite direction to that of magnetization direction of hard particles.

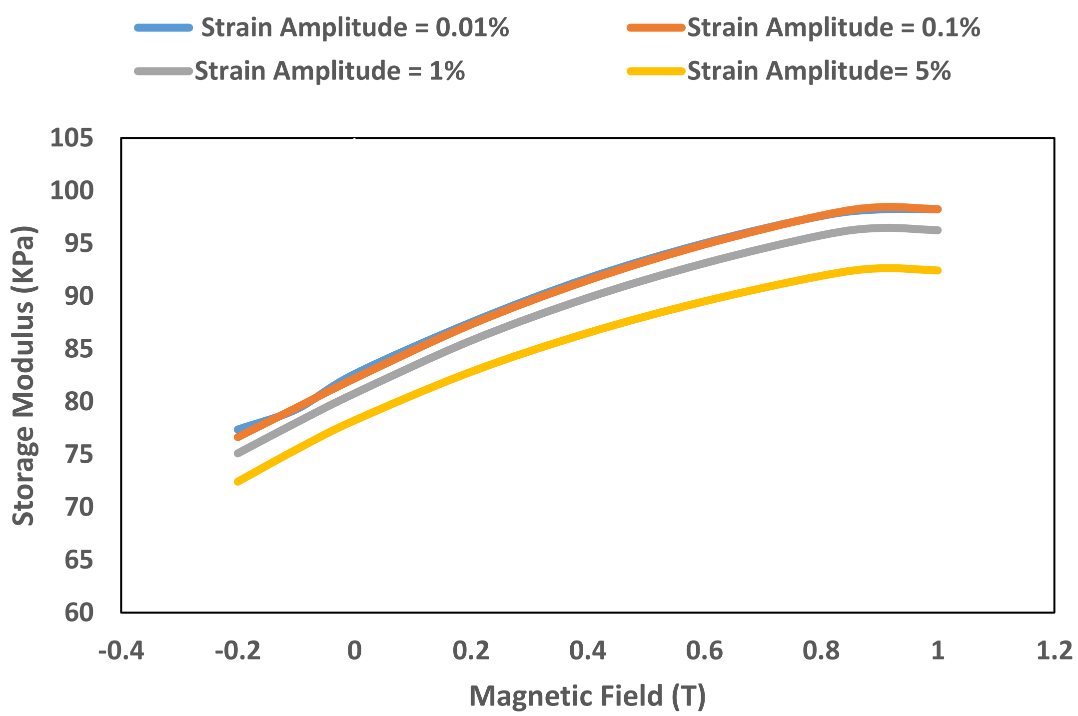

Figure 2-13. Dependence of storage modulus on the magnetic field at the frequency of 1 Hz for different shear strain amplitudes.

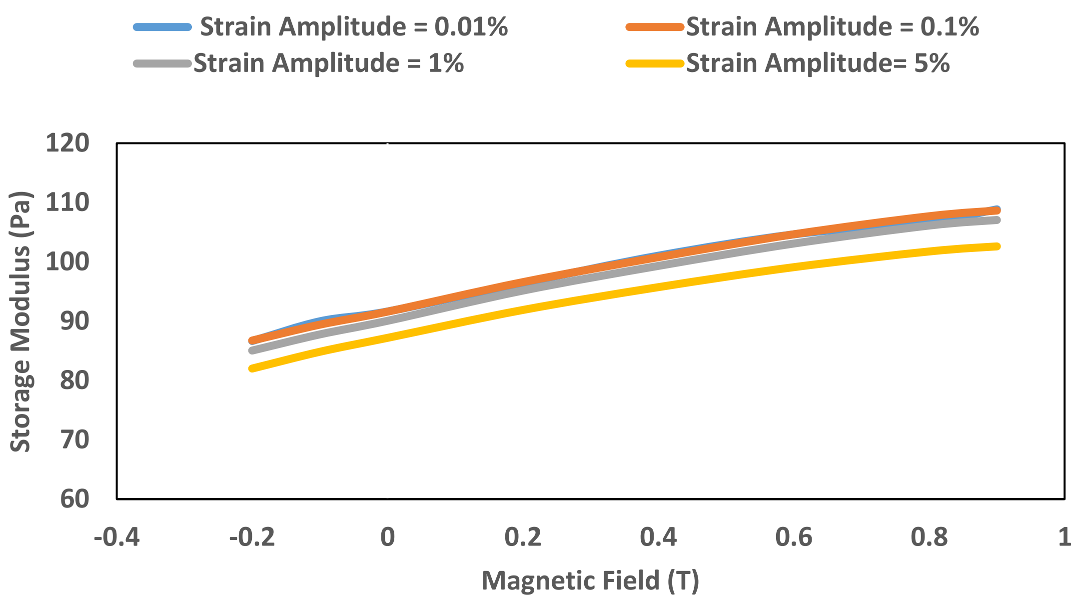

Figure 2-14. Dependence of storage modulus on the magnetic field at the frequency of 5 Hz for different shear strain amplitudes.

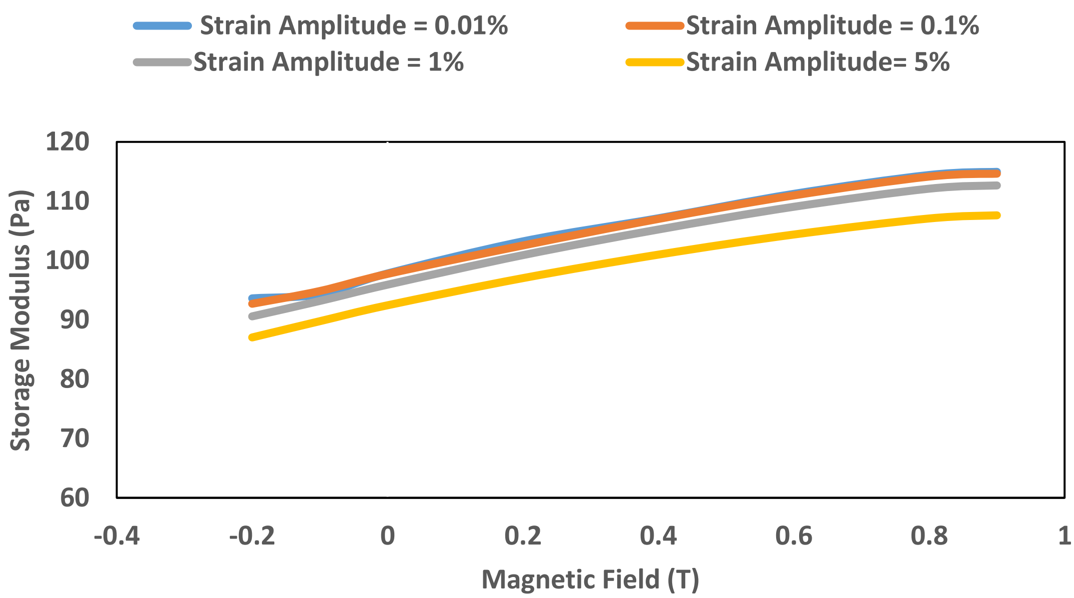

Figure 2-15. Dependence of storage modulus on the magnetic field at the frequency of 10 Hz for different shear strain amplitudes.

2.3.4 Viscoelastic behavior and Hysteresis loops

Owing to the viscoelastic nature, the MREs exhibit hysteresis-like stress-strain characteristics. The energy within a perfectly elastic material is completely recovered when the stress is removed. But the viscous element, which is caused by internal molecular friction, retards the elastic strain and results in loss of energy in material. This energy is dissipated in the form of heat in the elastomer. The amount of energy loss per cycle of strain is known as the hysteresis. The area under the loading curve is proportional to the energy input and the area under the unloading curve is proportional to the energy returned. Accordingly, the difference area, which is enclosed between loading and unloading path, is the hysteresis loss or equivalent damping. Additionally, the slope of hysteresis loops indicates the equivalent stiffness. The stress-strain or force-displacement hysteresis of MREs strongly depends on the input frequency, strain amplitude as well as applied magnetic field intensity (Kallio et al., 2007, Lokander et al., 2003). The captured hysteresis loops of H-MREs in simple shear mode under 5% shear strain amplitude at different magnetic field densities and excitation frequencies are illustrated in Figures 2-16 to 2-18. Results suggest independency of enclosed area from the applied magnetic flux density which is in accordance with the negligible influence of magnetic field on the loss modulus of the H-MRE presented in Figure 2-12. In contrary, the slope of the major axis of the hysteresis loop, representing the storage modulus of the H-MRE, clearly depends on the intensity of the applied magnetic field for all different driving frequency (1, 5, and 10 Hz) presented in Figures 2-16 to 2-18, respectively. It should be mentioned that by increasing the excitation frequency, from 1 Hz to 5 and 10 Hz, the intermolecular heat generated inside the H-MRE sample rises and consequently the energy dissipation (area inside the hysteresis loop) in the H-MRE increases by increasing the excitation frequency. This phenomenon appears as the growth in the loss modulus with respect to the frequency confirming the results in Figure 2-12.

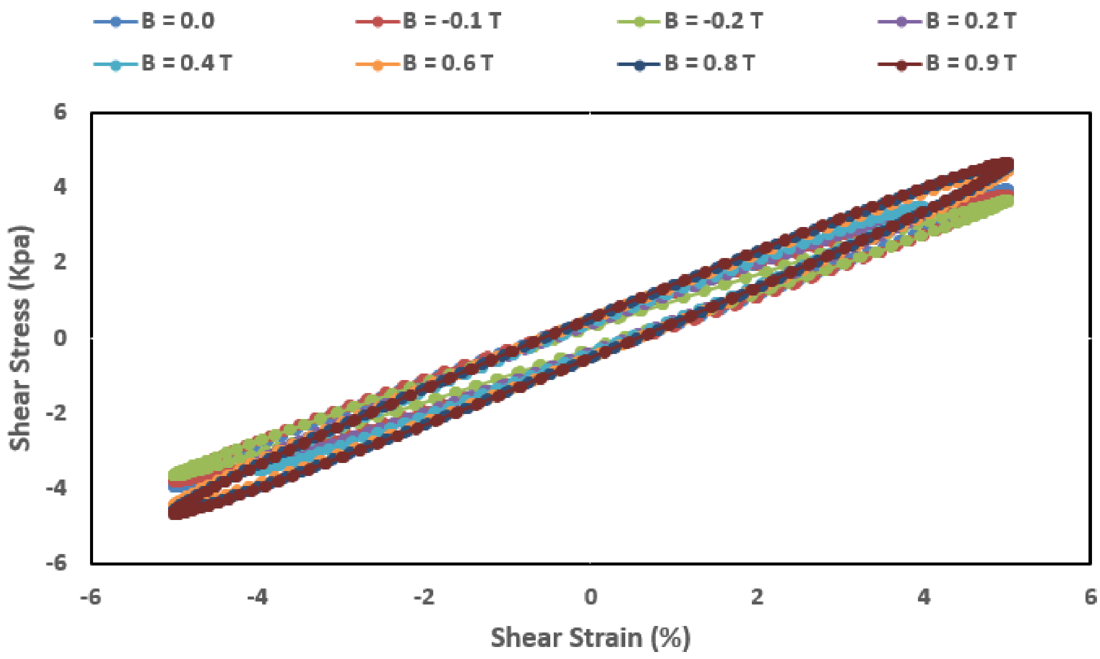

Figure 2-16. Hysteresis loop at 1 Hz frequency and 5 % Shear Strain for different magnetic field densities.

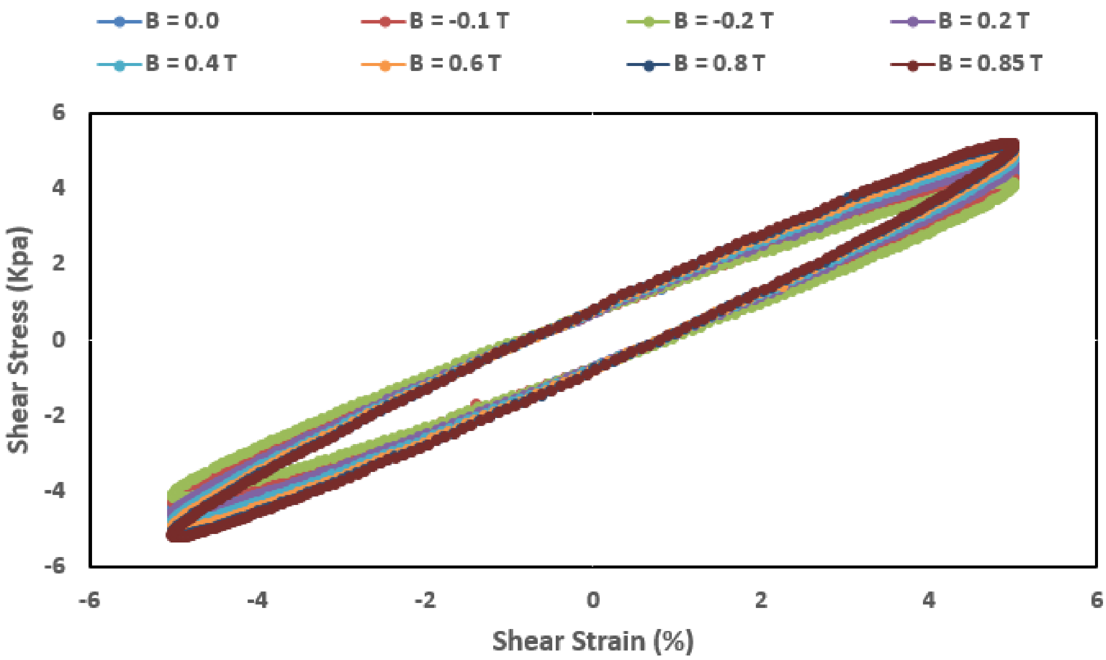

Figure 2-17. Hysteresis loop at 5 Hz frequency and 5 % Shear Strain for different magnetic field densities.

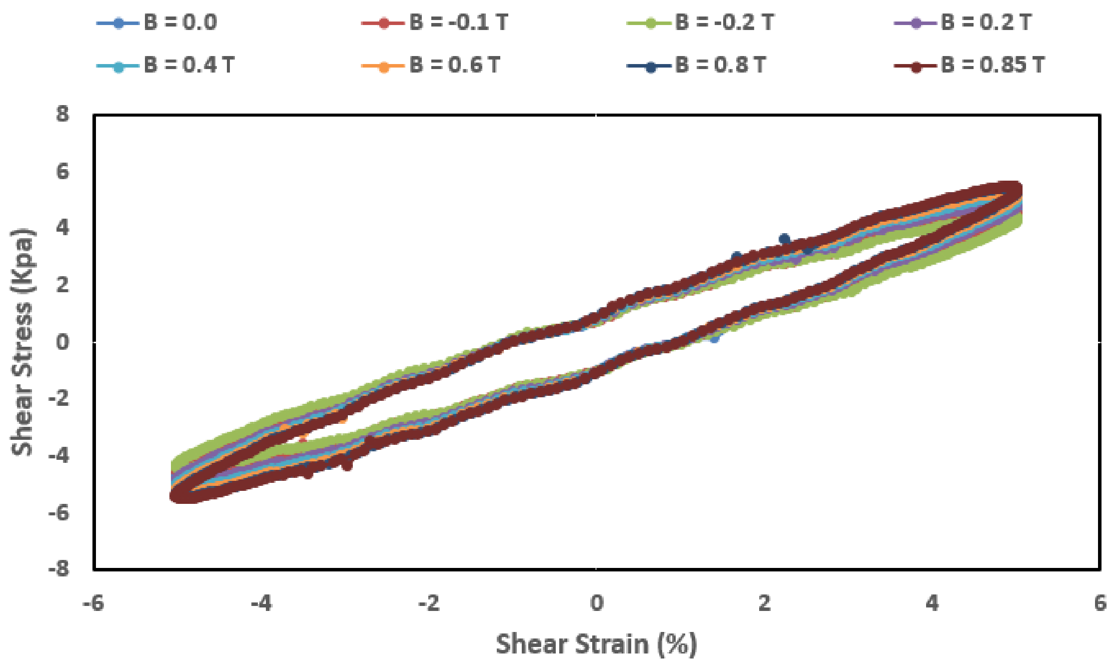

Figure 2-18. Hysteresis loop at 10 Hz frequency and 5 % Shear Strain for different magnetic field densities.

2.4 Conclusion

H-MRE samples with 15% volume fraction of hard magnetic particles were fabricated in the laboratory by mixing hard magnetic particles and silicone rubber matrix. The viscoelastic properties of the H-MRE were measured using an advanced rotary rheometer (Discovery HR-3, TA instrument) equipped with magnetorheology accessory. The test sample (20 mm diameter and 2 mm thickness) was placed between the rotating and fixed parallel plate geometries of the magnetorheometer. Dynamic tests were carried out in a wide range of frequencies, strain amplitude and magnetic field intensities. Effects of loading conditions and magnetic field intensity on both elastic and loss moduli of H-MREs were investigated and discussed. In order to investigate the influence of shear strain amplitude on the storage and loss moduli of H-MRE's, the oscillatory shear test were performed by sweeping the strain amplitude in the range of 0.01% to 5% , in the wide range of frequency, from 1 Hz to 20 Hz, while the temperature maintained steady at 20 °C. The tests were implemented under various levels of positive and negative applied magnetic flux density varied from B = -0.2 T to B=1 T to study the effect of applied magnetic field on the mechanical properties of the H-MRE. Moreover, sweep frequency tests have been performed in order to investigate the effect of excitation frequency on the behavior of H-MREs operating in shear mode. For this purpose, the oscillatory shear tests were conducted under constant strain amplitude of 0.01%, while the frequency was swept in the range of 0.1 to 60 Hz. The tests were performed under various magnitudes of applied magnetic flux densities ranging from -0.2 T to 0.85 T in order to investigate the effect of both negative and positive magnetic field on the dynamic behavior of H-MREs. It was shown that unlike the soft MREs, applying magnetic field in the direction opposite to the orientation of the magnetization weakens the magnetic bonding between the hard particles and consequently reduces the storage modulus of the H-MRE. Thus, it is possible to make the H-MRE softer or stiffer by changing the direction of magnetic field. On the other hand, results showed that changing the direction of the applied magnetic field does not noticeably affect the loss modulus of H-MRE and applying magnetic field in either direction slightly enhances the loss modulus of the H-MRE.

Chapter 3: Modeling of Dynamic Properties of H-MREs

3.1 Introduction

Modeling and understanding dynamic behavior of MREs under various loading conditions is essential to design appropriate MRE-based devices for vibration control. A number of studies have focused on developing models for predicting properties and dynamic behavior of MREs. These models are generally categorized as physics-based and phenomenological-based models. The physics-based models can be classified into two different branches. The first type of modeling is based on the continuum mechanics theory, employing finite strain theory to study the coupled mechanical and magnetic behavior of MREs (Beheshti et al., 2020). The second branch of physics-based models is based on the microstructure of MREs. The micro-structure based models utilize the interaction of dipole micron-size ferromagnetic particles to predict both the moduli and MR effect (Shen et al., 2004; Khanouki et al., 2019). The physics-based models, however, involve considerable simplifying assumptions and are generally independent of the strain amplitude and the strain rate (Davis., 1999, Shen et al., 2004). Moreover, for describing properties of different types of MREs, the generalization of physics-based models poses complexities due to widely different physical properties of the MREs. The phenomenological-based models of MREs are generally experiment based in which the model parameters are identified through the minimization of errors between simulated and experimental results at different strain rate and amplitude as well as applied magnetic field (Norouzi et al., 2015). Such phenomenological models to address the hysteresis behavior of MREs can be described using the polynomial or power functions (Norouzi et al., 2015) or Bouc-Wen formulation (Yang et al., 2013). Alternatively, operator-based phenomenological models such as Prandtl-Ishlinskii and Preisach models, are also widely reported for modeling of hysteresis in smart material actuators (Dargahi., 2017). Phenomenological-based models are efficient models that can be effectively utilized for development of model-based control strategies.

In this study phenomenological-based mathematical models are developed to predict the viscoelastic properties of the H-MRE with respect to the applied magnetic flux density and excitation frequency. The proposed models are then validated by comparing the predicted results with those obtained experimentally.

3.2 Model Formulation

Phenomenological-based mathematical models are developed to predict the viscoelastic properties of the H-MRE with respect to the applied magnetic flux density and excitation frequency. The model is developed for H-MREs operating in shear mode at linear viscoelastic region ($\gamma = 0.01$ %). The proposed models are capable of predicting the storage and loss moduli of H-MREs in presence of both negative and positive magnetic field (-0.2 to 0.85 T) and wide range of operating frequency (1 to 50 Hz).

Through examination of results presented in Figures 2-11 and 2-12, one can realize that variation of the storage and loss moduli of the H-MRE with respect to the driving frequency can be represented by power functions. This observation stems from the fact that the storage and loss moduli increase almost linearly versus excitation frequency in the logarithmic scale as shown in these figures. The mathematical models for the storage and loss moduli are, thus, proposed to be in the following form:

$$G'(f) = a_B f^{b_B} \tag{3.1}$$

$$G''(f) = c_B f^{d_B} \tag{3.2}$$

Where $G'(f)$ and $G''(f)$ are storage and loss moduli in Pa, respectively, and f represents the excitation frequency in Hz. a_B, b_B, c_B, and d_B are field dependent parameters which should be determined for each applied magnetic flux density using the experimental results. For this purpose, the error function between the results obtained using the developed model and those obtained experimentally are minimized using the least square method. The error function can be expressed as:

$$J_{G'} = \sum_{i=1}^{M} (G'_{Model}(i) - G'_{Exp.}(i))^2 \tag{3.3}$$

$$J_{G''} = \sum_{i=1}^{M} (G''_{Model}(i) - G''_{Exp.}(i))^2 \tag{3.4}$$

In which subscripts $_{Exp.}$ and $_{Model}$ represent the experimental results and those obtained using the developed model, respectively. For each magnetic flux density, two parameters, a_B and b_B for storage modulus and c_B and d_B for loss modulus are identified through the minimization of the error functions in Eqs. (3.3) and (3.4). These parameters are listed in Table 3-1. It should be noted that the proposed power functions in Eqs. (3.1) and (3.2) are capable of predicting the moduli in the range of 1 to 50 Hz accurately.

Table 3-1. Field dependent parameters in the developed models at various applied magnetic flux densities.

Magnetic flux density (T)	a_B	b_B	c_B	d_B
-0.2	7.787e+04	0.09197	9452	0.2263
-0.1	8.069e+04	0.08805	9463	0.2229
0.0	8.421e+04	0.08321	9575	0.22
0.2	8.975e+04	0.07845	9845	0.2151
0.4	9.397e+04	0.07717	1.008e+04	0.212
0.6	9.73e+04	0.075	1.028e+04	0.2098
0.8	1.004e+05	0.07579	1.061e+04	0.2096
0.85	1.01e+05	0.07573	1.065e+04	0.2092

Figure 3-1 shows the variation of the obtained parameters with respect to the applied magnetic flux density.

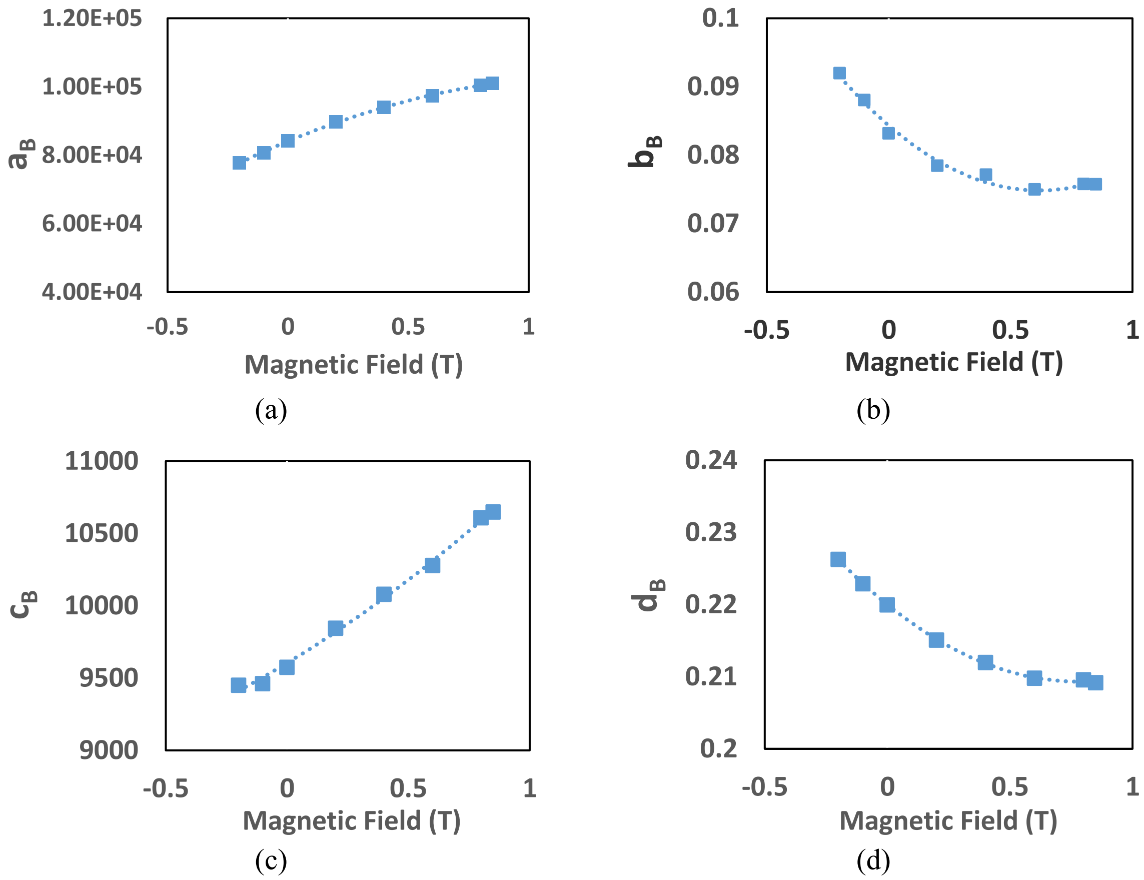

Figure 3-1. Variation of the parameters (a) a_B, (b) b_B, (c) c_B, and (d) d_B with respect to the applied magnetic flux density: the square (experiment), the dotted curve (model).

Examination of Figure 3-1 suggests that a second order polynomial function can be effectively utilized to quantify these parameters as a function of applied magnetic flux density as follows:

$$a_B = a_{B_2}B^2 + a_{B_1}B + a_{B_0} \tag{3.5}$$

$$b_B = b_{B_2}B^2 + b_{B_1}B + b_{B_0} \tag{3.6}$$

$$c_B = c_{B_2}B^2 + c_{B_1}B + c_{B_0} \tag{3.7}$$

$$d_B = d_{B_2}B^2 + d_{B_1}B + d_{B_0} \tag{3.8}$$

where B is the applied magnetic flux density in T. $a_{B_{0,1,2}}$, $b_{B_{0,1,2}}$, $c_{B_{0,1,2}}$, and $d_{B_{0,1,2}}$ are the parameters which are identified by minimizing the error function obtained as the difference between parameters presented in Table 3-1 and those calculated using Eqs. (3.5) to (3.8). Table 3-2 provides the identified parameters.

As it can be seen in Figure 3-1, the proposed quadratic functions presented in Eqs. (3.5) - (3.8) can accurately predict the variation of the parameters in the whole range of applied flux densities. Finally, by substituting Eqs. (3.5) and (3.6) into Eq. (3.1) and Eqs. (3.7) and (3.8) into Eq. (3.2) and using the parameters presented in Tables 3-2, the following equations can be obtained for the storage and loss moduli of the H-MRE:

$$G'(B,f) = (a_{B_2}B^2 + a_{B_1}B + a_{B_0})f^{(b_{B_2}B^2 + b_{B_1}B + b_{B_0})} \tag{3.9}$$

$$G''(B,f) = (c_{B_2}B^2 + c_{B_1}B + c_{B_0})f^{(d_{B_2}B^2 + d_{B_1}B + d_{B_0})} \tag{3.10}$$

In the following section it has been shown that the proposed models can accurately predict the storage and loss moduli of the H-MRE under wide range of applied excitation frequency and magnetic flux densities.

Table 3-2. Identified parameters in Eqs. (3.5) - (3.8).

a_{B_0}=84068	b_{B_0}=0.0843	c_{B_0}=9596.1	d_{B_0}=0.22
a_{B_1}=29271	b_{B_1}=-0.0307	c_{B_1}=956.6	d_{B_1}=-0.0275
a_{B_2}=-11136	b_{B_2}=0.0249	c_{B_2}=352.97	d_{B_2}=0.0177

3.3 Validation of the Developed Models

In this section, the results obtained using the developed phenomenological-based models are compared with those measured experimentally to evaluate the performance of the proposed models. Figures 3-2 and 3-3 show the results for the storage and loss moduli with respect to the applied magnetic flux density at various excitation frequencies, respectively. Results clearly show that the moduli obtained from the proposed models agree very well with those obtained experimentally and thus the model can accurately predict the storage and loss moduli under different loading conditions.

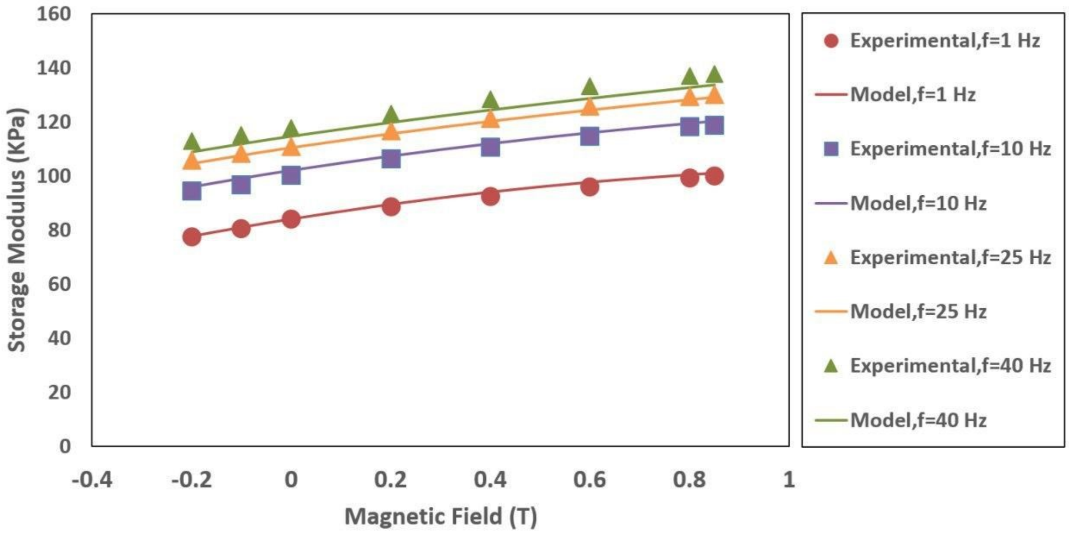

Figure 3-2. Comparison of the storage modulus predicted by the proposed model with those measured experimentally.

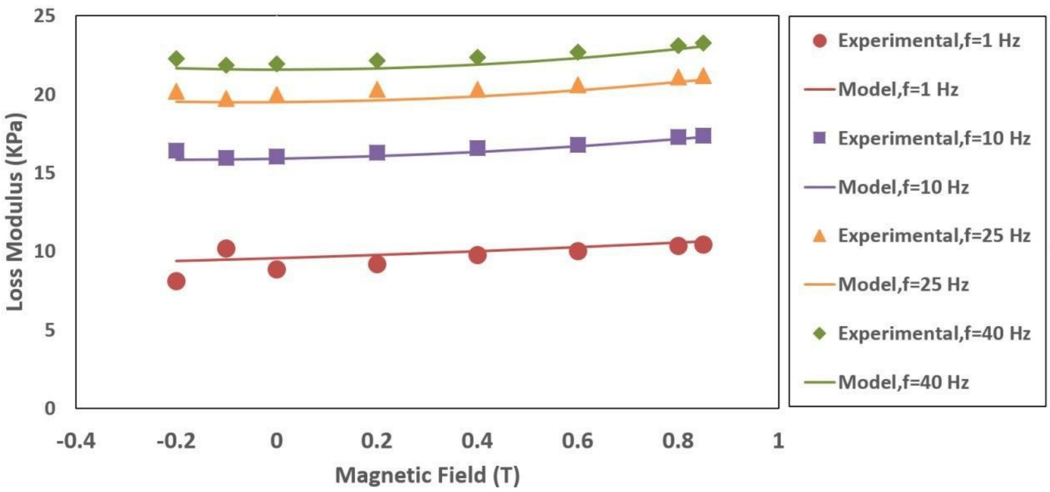

Figure 3-3. Comparison of the loss modulus predicted by the proposed model with those measured experimentally.

Comparing Figures 3-2 and 3-3 also confirm that that the dependency of the loss modulus on the applied magnetic flux density is negligible compared with the influence of the field variation on the storage modulus.

The variation of the storage and loss moduli with driving frequency also presented in Figures 3-4 and 3-5, respectively, in which the results obtained using proposed models are compared with those measured experimentally. As it can be realized, the proposed models can accurately capture the behavior of the H-MRE versus excitation frequency for both positive and negative magnetic fields. The model prediction is completely in accordance with the experimental results especially in the range of 1-30 Hz while slightly deviated from the experiential results at higher frequencies.

For further evaluation of the developed model, the coefficients of determination (R^2) is also calculated as the difference between the storage or loss modulus predicted by the proposed models and those obtained from the experiments to quantify the error as:

$$R^2 = [1 - \frac{\sum(G_{Model} - G_{Exp})^2}{\sum[G_{Model} - mean(G_{Exp})]^2}] \times 100 \tag{3.11}$$

Where G represent the storage or loss modulus of the H-MRE. It is noted that (R^2) varies between 0 and 100% in which 1 (100%) represents perfect fit. Table 3-3 shows the results for the coefficient of determination for different applied magnetic flux densities in the frequency range of 1-50 Hz. As it can be realized for all cases R^2 is generally over 95% suggesting that the proposed models can accurately capture the dynamic viscoelastic behavior of the H-MRE.

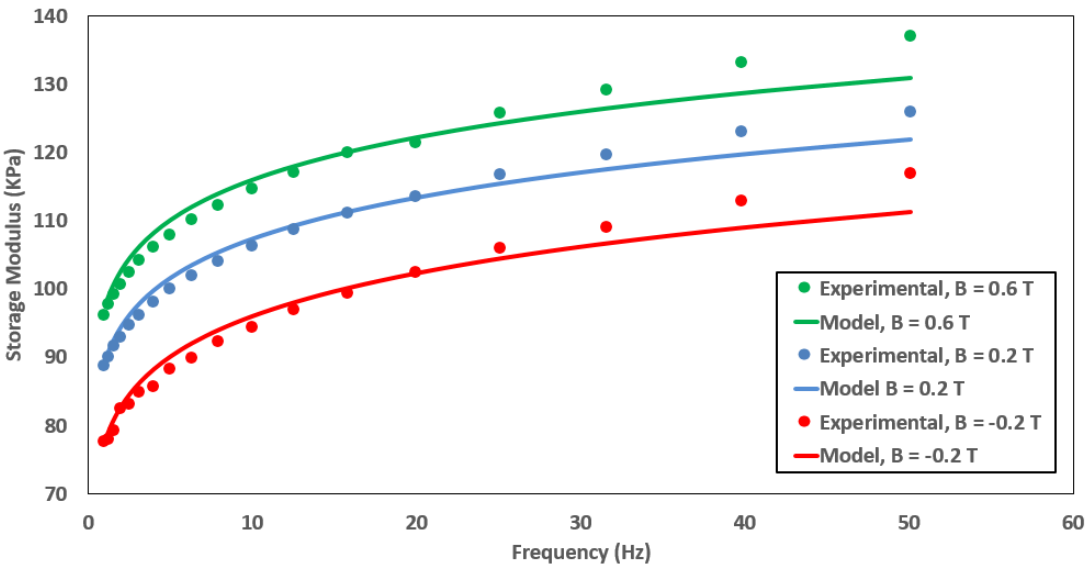

Figure 3-4. Comparison of the storage modulus versus frequency predicted by the proposed model with those measured experimentally.

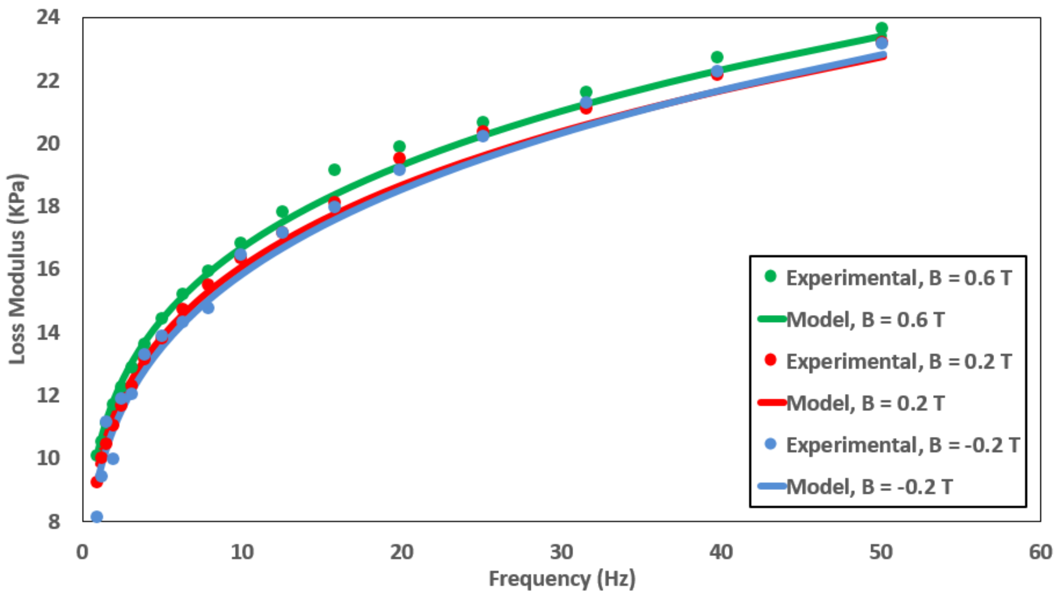

Figure 3-5. Comparison of the loss modulus versus frequency predicted by the proposed model with those measured experimentally.

Table 3-3. The coefficient of determination, R^2, or both the storage and the loss moduli under different magnetic flux densities.

Magnetic field (T)	R^2 (for the storage modulus)	R^2 (for the loss modulus)
B = -0.2	96.51	98.24
B = -0.1	95.80	98.79
B = 0.0	96.35	99.15
B = 0.2	97.59	99.09
B = 0.4	96.52	99.38
B = 0.6	95.84	99.45

The percentage error is also employed to find the relative error between simulation and experimental results at different applied magnetic flux density and driving frequency. Tables 3.4 and 3.5 presents the percentage error for the storage and the loss moduli, respectively. The range of the percentage error for the storage modulus is from 0.01 % to 4.74 %, and the average of the percentage error is almost 2.37 %. For the loss modulus, the range of the percentage error is from 0 % to 9.4 %, and the average of the percentage error is nearly 4.7 %. In general, for the majority of cases the average percentage error between the experimental and model results is below 3%. The percentage errors shown in these tables further confirm the accuracy of the models to predict the moduli of MREs in a wide range of applied magnetic flux density and driving frequency.

Table 3-4. Percentage error of the storage modulus for different magnetic fields and frequencies.

	f **= 1 Hz**	***f*** **= 5 Hz**	***f*** **= 10 Hz**	***f*** **= 20 Hz**	***f*** **= 40 Hz**	***f*** **= 50 Hz**
B = -0.2 T	0.32	2.24	1.72	0.15	3.42	4.74
B = -0.1 T	0.66	3.23	2.5	0.28	2.9	4.29
B = 0.0 T	0.57	2.66	2.13	0.52	2.77	3.96
B = 0.2 T	0.96	1.7	1.06	0.01	2.54	3.02
B = 0.4 T	0.01	0.01	1.07	1.13	1.19	1.21
B = 0.6 T	1.67	2.1	1.21	0.59	3.4	4.44

Table 3-5. Percentage error of the loss modulus for different magnetic fields and frequencies.

	f **= 1 Hz**	***f*** **= 5 Hz**	***f*** **= 10 Hz**	***f*** **= 20 Hz**	***f*** **= 40 Hz**	***f*** **= 50 Hz**
B = -0.2 T	9. 4	2.15	3.36	3.08	2.62	1.31
B = -0.1 T	0.02	0	0	0.01	0.01	0
B = 0.0 T	8.4	1.78	0.63	1.17	1.62	1.19
B = 0.2 T	6.4	0.71	1.38	4.25	2.19	1.84
B = 0.4 T	2.73	0.48	1.48	3.83	2.06	1.04
B = 0.6 T	0.01	1.89	2.65	4.65	3.44	2.55

3.4 Conclusion

A field-dependent phenomenological model was formulated to predict the variation of storage and loss moduli of H-MREs under varying excitation frequency and applied magnetic flux density. The model is developed for the H-MRE with 15% volume fraction of hard particles operating in shear mode at linear viscoelastic region ($\gamma = 0.01$ %). The measured data was used to identify the parameters of this phenomenological model through minimization of the error function between the model and the measured responses over the wide range of driving frequency and in presence of both negative and positive magnetic fields. The identified parameters of this phenomenological-based mathematical model showed dependence on the applied magnetic field intensity. Validity of the proposed model was examined by comparing the model responses with the measured data over the entire range of frequencies and magnetic flux densities. The coefficient of determination (R^2) between the model results and the measured data were generally observed to be above 95% for the storage and 98% for the loss modulus. According to the results, the proposed models can accurately predict the variation of storage and loss moduli under wide range of excitation frequencies (1 to 50 Hz) and in presence of both positive and negative magnetic fields (-0.2 to 0.85 T).

Chapter 4: Developing simple H-MRE based Vibration isolator

4.1 Introduction

The isolation systems have been intensively studied and used in high-precision measurement, automotive suspension, and disaster prevention systems to reduce environmental disturbances (Yoshioka et al., 2001; Yang et al., 2014). Environmental disturbances largely come from the ground vibrations transferred by the support system, in which increasing structural flexibility by adding small-stiffness isolation system is a main method for protecting engineering structures or equipment. The conventional vibration isolation systems are generally effective at a specified tuned frequency or at a very narrow frequency band around the tuned frequency which is typically specified at the early stages of design. Under varying excitation frequency outside the specified narrow frequency range, these passive systems will lose their control authority and even may increase the system response in untuned conditions. Fully active systems utilizing active actuators such as voice coil and piezoceramic can isolate the vibration over broad range of frequencies. While fully active systems have shown superior performance gain over the passive systems, they generally require a large power and complex and costly control hardware. MRE-based vibration isolators or absorbers are basically semi-active devices which have the reliability and fail-safe feature of passive systems while can also provide adaptability of fully active systems without large power requirement and complex control systems. As mentioned in Chapter 1, while S-MRE based devices have been widely studied, there is a very limited study on H-MRE based devices for vibration control applications. The objective of this chapter is to investigate the capability of the H-MRE to isolate the vibration under broad range of frequencies through the variation of the applied magnetic flux density. In the following, a tunable vibration isolator based on H-MRE is developed and modeled as a simple single-degree-of-freedom system to assess the capability of H-MRE-based isolators in isolating vibration under varying harmonic excitation. Moreover, the effect of both positive and negative magnetic fields on the transmitted vibration is investigated.

4.2 Design of Vibration Isolator

The schematic of the proposed H-MRE-based vibration isolator is shown in Figure 4-1. The MRE-based vibration isolator consists of: C-shape magnetic core conductor, magnetic coil, two H-MRE samples, shear plate and mounting plate connecting the payload to MREs. As it can realized, H-MREs are connected to the payload through a rigid shear plate and are under direct shear due to the load exerted by the payload. The C-Shaped core intensifies and guides the magnetic flux generated by two magnetic coils through the H-MREs. It is noted that the direction of the magnetic field in the H-MREs is perpendicular to the vertical shear motion. The magnetic field intensity generated by the two coils, which installed around the core, can be directly controlled by the applied current to the coils.

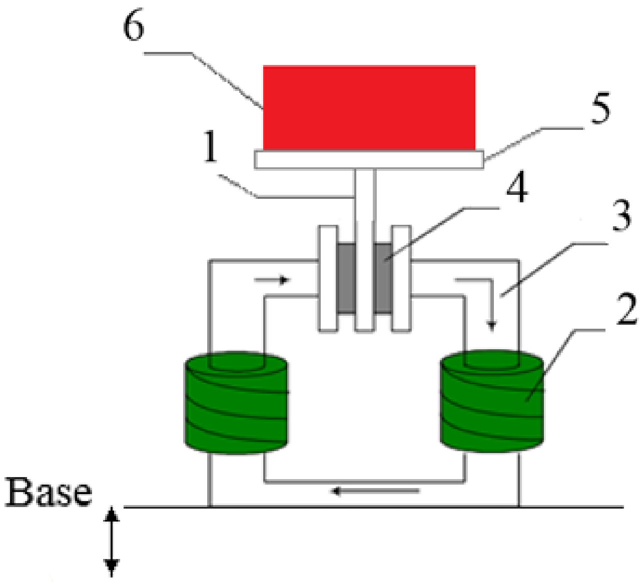

Figure 4-1. Sketch of the H-MRE-based vibration isolator: 1. Shear plate; 2. magnetic coil; 3. magnetic conductor; 4. MRE; 5. mounting plate; 6. Payload.

Figure 4-2 shows a schematic of electromagnet utilized in the design of the proposed isolator. As discussed above, when the electric current is supplied to the coils, the generated magnetic flux is guided through the core and pass through H-MRE specimen placed in the gap of the C-shape core frame as shown in Figure 4-2. Through the application of the magnetic field, the shear modulus of H-MREs can be instantly and reversibly changed, thus the natural frequency of the isolator can be varied adaptively through direct variation of the current applied to the electromagnet.

An ideal magnetic circuit aims at providing a low reluctance flux conduit to guide and intensify the magnetic flux into region where H-MRE resides; maximizing the magnetic field energy in the H-MRE, while in the meantime minimizing the energy loss in the underutilized areas and finally maintaining sufficient cross section of steel core to keep the magnetic field intensity, H, in the steel very low while minimizing the weight of the steel core (Fan Lin, 2019).

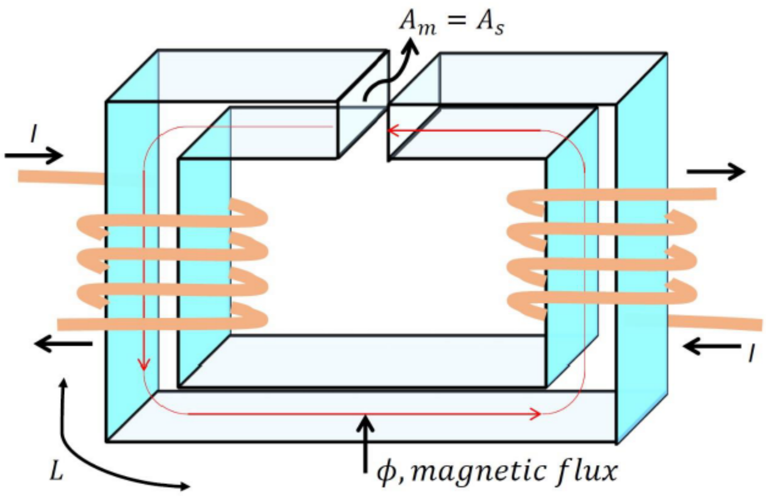

Figure 4-2. Schematic of an electromagnet (Fan Lin, 2019).

In the following, the general procedure of designing magnetic circuit in MR based devices is briefly explained. First, the required operating magnetic flux density, B_m in the given B-H curve of H-MRE is selected. It is noted that the magnetic flux in the H-MRE specimen can be obtained as $\emptyset_m = B_m A_{H-MRE}$ in which B_m is the required magnetic flux density in the H-MRE and A_{H-MRE} is the cross- sectional area of the H-MRE. Then, the magnetic flux density is evaluated in the steel core conduit by applying the conservation of the magnetic flux density in the magnetic circuit as:

$$\emptyset_m = B_m A_{H-MRE} = B_s A_s \rightarrow B_s = \frac{\emptyset_m}{A_s} = \frac{B_m A_{H-MRE}}{A_s} \tag{4.1}$$

Having these parameters, the magnetic field intensity is determined in the steel core, H_s, using evaluated B_s and available B-H curve for steel. Subsequently, the required amp-turns can be obtained utilizing the Ampere's law as:

$$\oint hdl = NI \rightarrow H_m * 2h_{H-MRE} + H_s * L = NI \tag{4.2}$$

In which h_{H-MRE} is the thickness of the H-MRE specimen, L is the total length of the flux going through the C-shape steel conduit, N is the total turns of coils in the circuit, I is the input current, H_m is the magnetic field in H-MREs and H_s is the magnetic field in the steel.

The H-MRE samples, were connected to the mounting plate by a rigid shear plate. To ensure that MREs operate in linear viscoelastic region, the shear deformation experienced by MREs should be under 0.1%. As discussed before, this would be desirable as in the linear viscoelastic region, the storage modulus of MREs is independent of the strain amplitude. By increasing the strain amplitude, MREs exhibit nonlinear viscoelastic behavior causing drastic reduction in storage modulus which is not desirable. It has been found that under payload mass of 15 kg, the H-MRE samples with the size of 0.1 $m \times 0.1$ m and thickness of 0.01 m would experience quasi-static shear deformation under 0.1% for minimum applied magnetic field of -0.2 T (worse case in which storage modulus of the MRE is the lowest).

The MRE geometrical parameters and mass of the payload which will be used in subsequent section are summarize in Table 4-1.

Table 4-1. Assumed parameters of H-MRE and mass of the payload.

A_{H-MRE}	0.01 m^2
h_{H-MRE}	0.01 m
$m_{payload}$	15 Kg

4.3 Modeling the vibration isolator as a single-degree-of-freedom system

The mathematical model of a vibration isolation system can be represented by a single-degree-of-freedom system as shown in Figure 4-3.

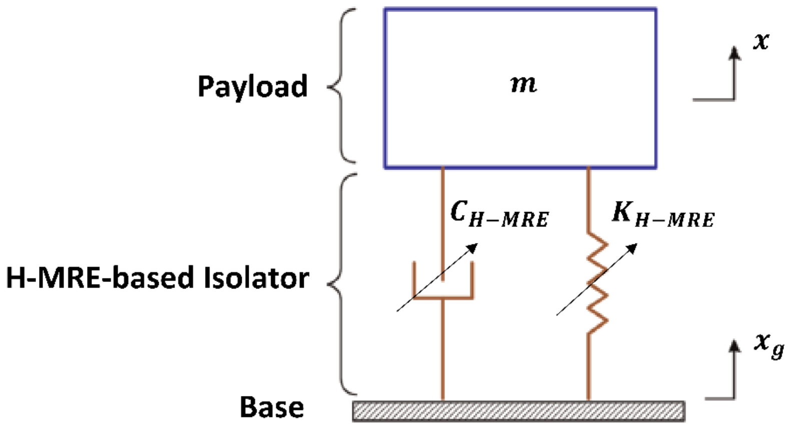

Figure 4-3. A schematic of a single-degree-of-freedom system (Liao et al., 2012).

As shown in Figure 4-3, m is the mass of the payload; C_{H-MRE} and K_{H-MRE} are the field dependent equivalent damping coefficient and the stiffness of the H-MRE isolator, respectively and x and x_g are the displacements of the payload and the ground base, respectively. The governing equation of the system can be described as:

$$m\ddot{x} + C_{H-MRE}\dot{x} + K_{H-MRE}x = C_{H-MRE}\dot{x}_g + K_{H-MRE}x_g \tag{4.3}$$

Figure 4-4 shows a schematic of H-MRE sample under shear deformation. Considering this figure, under the application of shear force, F_s, the shear stress and shear strain in the H-MRE are obtained as follows:

$$\tau_s = \frac{F_s}{A_{H-MRE}} \tag{4.4}$$

$$\gamma_s = \frac{x_s}{h_{H-MRE}} \tag{4.5}$$

Where τ_s and γ_s represent the shear stress and shear strain in the H-MRE sample, respectively. A_{H-MRE} is the cross- sectional area of the H-MRE and h_{H-MRE} is its thickness. Considering, the linear viscoelasticity, the shear stress and shear strain could be related as:

$$\tau_s = G_{H-MRE}\gamma_s \tag{4.6}$$

Where G_{H-MRE} is the complex shear modulus of the H-MRE which can be written as:

$$G_{H-MRE} = G'_{H-MRE} + iG''_{H-MRE} \tag{4.7}$$

Where G'_{H-MRE} and G''_{H-MRE} are the storage and loss moduli of the H-MRE operating in linear viscoelastic region, respectively. Using Eqs. (4.5) - (4.7), Eq. (4.4) can be written as:

$$F_s = \left(\frac{A_{H-MRE}G'_{H-MRE}}{h_{H-MRE}} + i\frac{A_{H-MRE}G''_{H-MRE}}{h_{H-MRE}}\right)x_s \tag{4.8}$$

For a harmonic excitation, F_s can be written as a function of equivalent stiffness and damping coefficient of H-MRE as follows:

$$F_s = \bar{K}_{H-MRE}(x_s) + \bar{C}_{H-MRE}(i\omega x_s) \tag{4.9}$$

Where ω is the excitation frequency in rad/s. Comparing the Eqs. (4.8) and (4.9) the equivalent stiffness and damping of the H-MRE sample are obtained as:

$$\bar{K}_{H-MRE} = \frac{G'_{H-MRE}A_{H-MRE}}{h_{H-MRE}} \tag{4.10}$$

$$\bar{C}_{H-MRE} = \frac{G''_{H-MRE}A_{H-MRE}}{\omega h_{H-MRE}} \tag{4.11}$$

Looking into Figure 4-1, two H-MRE specimens have been utilized in the H-MRE-based isolator. Therefore, the equivalent stiffness and damping coefficient in Eq. (4.3) are twice the values obtained from Eqs. (4.10) and (4.11):

$$K_{H-MRE} = \frac{2G'_{H-MRE}A_{H-MRE}}{h_{H-MRE}} \tag{4.12}$$

$$C_{H-MRE} = \frac{2G''_{H-MRE}A_{H-MRE}}{\omega h_{H-MRE}} \tag{4.13}$$

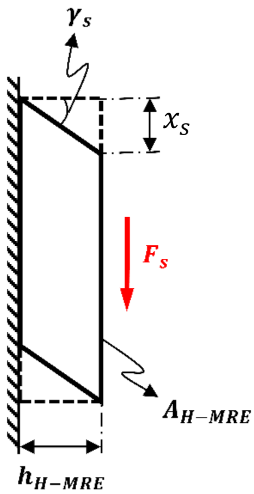

Figure 4-4. A schematic of the H-MRE sample under shear deformation.

The transmissibility of the system (ratio of the payload amplitude displacement or acceleration to the ground amplitude displacement or acceleration) can be written as:

$$T = \frac{X}{X_g} = \frac{A}{A_g} = \sqrt{\frac{1 + (2\lambda\xi)^2}{(1-\lambda^2)^2 + (2\lambda\xi)^2}} \tag{4.14}$$

In which X, X_g, $A = \omega^2 X$ and $A_g = \omega^2 X_g$ are payload displacement amplitude, ground displacement amplitude, payload acceleration amplitude and ground acceleration amplitude, respectively and natural frequency, ω_n, frequency ratio, λ, and damping factor , ξ, are defined as:

$$\omega_n = \sqrt{\frac{k}{m}} \quad , \qquad \lambda = \frac{\omega}{\omega_n} \qquad , \quad \xi = \frac{C}{C_c} = \frac{C}{2\sqrt{km}} \tag{4.15}$$

It should be noted that the natural frequency, ω_n, is defined as the natural frequency of the isolator in absence of magnetic field ($B = 0\ T$).

4.4 Discussion and Results

The transmissibility curves with respect to frequency ratio for frequency range from 1 Hz to 10 Hz under different applied magnetic flux densities are shown in Figure 4-5. The natural frequency of the isolator in the absence of the applied magnetic field is 6.4 Hz. As it can be realized, the transmissibility curves for 0.8 T and 0.85 T are very close, which indicates the possible saturation of the MR elastomer nearly around 0.8 T. The natural frequency of the MRE base isolator and their associated peak transmissibly increases from 6.2 Hz to 7 Hz and 6.5 to 7.3, respectively by increasing the magnetic flux density from -0.2 T to 0.8 T. It is noted that the equivalent viscous damping is inversely proportional to the frequency according to Eq. 4.11. Thus, by increasing the natural frequency of the system due to increase in applied flux density, the amount of the equivalent viscous damping coefficient decreases leading to higher transmissibility. Results show that in the absence of the applied magnetic flux density, the passive isolator has a very poor vibration isolation performance at excitation frequency very near to the natural frequency of the passive isolator (6.4 Hz) with high peak transmissibility of 6.8. By decreasing the magnetic flux density to -0.2 T, the transmissibility significantly decreases to 6.5, which is almost 4.4 % reduction in transmitted vibration to the payload.

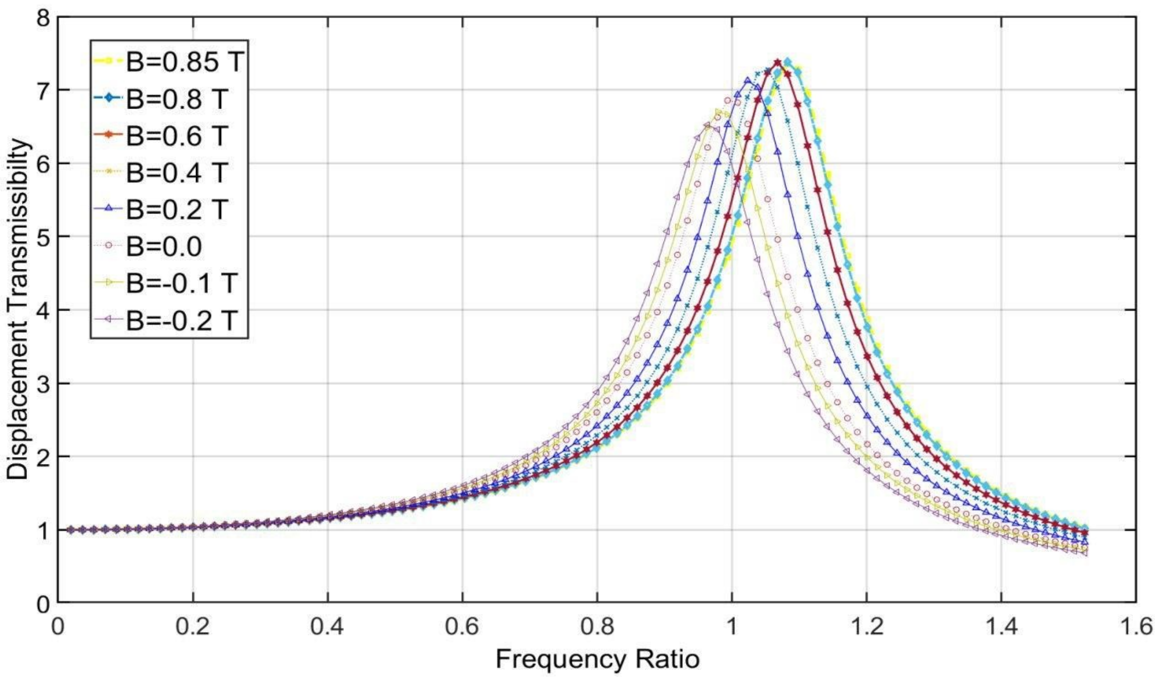

Figure 4-5. Transmissibility of a single-degree-of-freedom system for wide range of magnetic field, from B= -0.2 T to B= 0.85 T.

To better realize the potential of H-MREs, Figure 4-6 shows the transmissibility curves of the H-MRE isolator for the most negative (-0.2 T) and the most positive (0.85 T) applied flux densities considered in this study. The crossing excitation frequency corresponding to the intersection point between these two curves is 6.6 Hz. As it can realized, before the intersection point the low transmissibility occurs under positive flux density of 0.85 T while after the intersection point, the low transmissibility occurs under negative flux density of -0.2 T. It is interesting to note that under low and negative applied flux density, the high frequency vibration can be effectively isolated with low power compared with positive flux density of 0.85 T. This observation may provide an essential guidance to design an effective, yet simple, semi-active control strategy to isolate the vibration under broad-band frequency range. This may be achieved by measuring the excitation frequency and utilize a semi-active on-off control strategy to apply maximum positive and negative flux density if the excitation frequency is lower and higher than the crossing excitation frequency, respectively. Thus, compared with S-MRE in which the equivalent stiffness of the MRE only increases irrespective of the direction of the applied magnetic field, H-MREs enable to provide negative stiffness effect and thus considerably enhance the control authority of the H-MRE-based isolator over wider range of frequency.

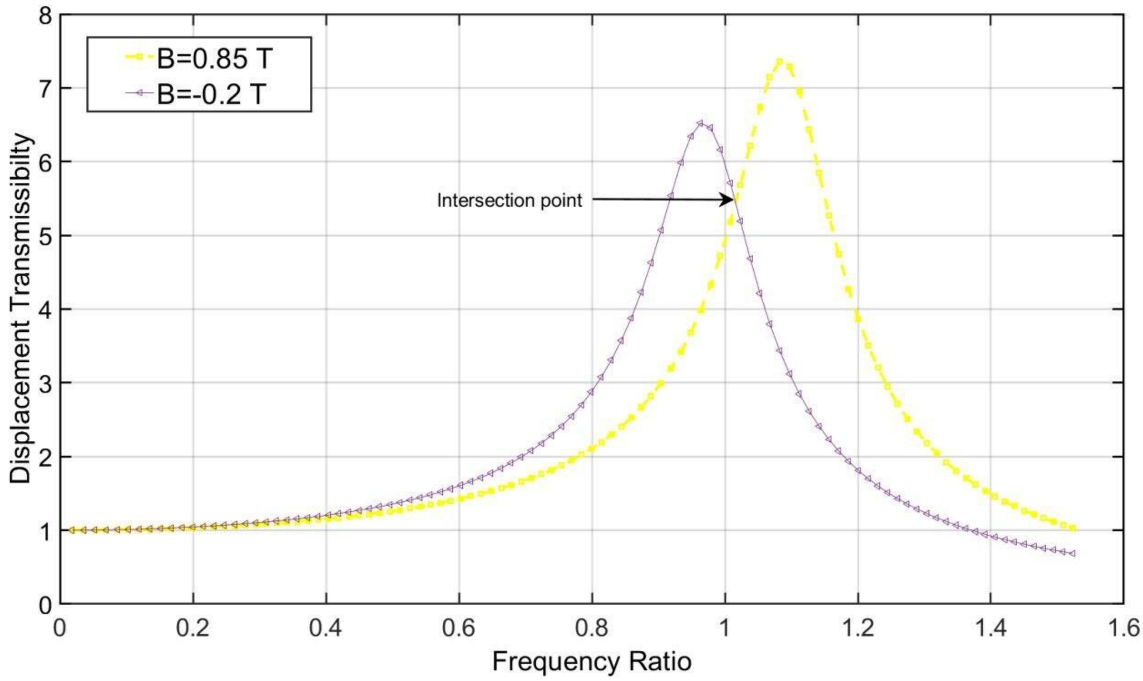

Figure 4-6. Transmissibility of a single-degree-of-freedom system for B= -0.2 T and B= 0.85 T.

4.5 Conclusion

In this chapter a tunable vibration isolator based on H-MRE is developed. First, the main parts of vibration isolator and the general procedure of designing magnetic circuit in MR based devices were briefly explained. Then, the vibration isolator was modeled as a single-degree-of-freedom system in order to evaluate its transmissibility under varied applied magnetic flux density. The results show that with a lower and negative magnetic flux density after a specific excitation frequency, the vibration can be effectively isolated compared with the positive magnetic field. Finally, it is showed that by adopting the proper semi-active control strategy and considering the both positive and negative magnetic fields, the bandwidth of the H-MRE based adaptive devices could be considerably enhanced.

Chapter 5: Conclusion, Contribution and Recommendations for future works

5.1 Conclusion

This dissertation aimed to provide an investigation on the magneto-mechanical characteristics of a new class of smart materials, namely magnetorheological elastomers based on hard particles (H-MREs). First, the H-MRE samples with 15% volume fraction of hard magnetic particles were fabricated in the laboratory by mixing hard magnetic particles and silicone rubber matrix. The viscoelastic properties of the H-MRE were measured using an advanced rotary rheometer (Discovery HR-3, TA instrument) equipped with magnetorheology accessory. The test sample (20 mm diameter and 2 mm thickness) was placed between the rotating and fixed parallel geometries. The number of dynamic tests were carried out in a wide range of frequencies, strain amplitude and magnetic field intensities. Effect of loading conditions and magnetic field intensity on both elastic and loss moduli of H-MREs were investigated and interpretation of experimental results were presented in details. In order to investigate the influence of shear strain amplitude on the storage and loss moduli of H-MRE's, the oscillatory shear test were performed by sweeping the strain amplitude in the range of 0.01% to 5% , in the wide range of frequency, from 1 Hz to 20 Hz. The tests were implemented under various levels of positive and negative applied magnetic flux density varied from B = -0.2 T to B=1 T to study the effect of applied magnetic field on the mechanical properties of the H-MRE. It was shown that unlike the soft MREs, applying magnetic field in the direction opposite to the orientation of the magnetization weakens the magnetic bonding between the hard particles and consequently reduces the storage modulus of the H-MRE. Thus, it is possible to make the H-MRE softer or stiffer by changing the direction of magnetic field. This behavior provides a unique opportunity to utilize H-MREs in different vibration control applications in which both negative and positive variation of the stiffness is required. Moreover, sweep frequency tests have been performed in order to investigate the effect of excitation frequency on the behavior of H-MREs operating in shear mode. For this purpose, the oscillatory shear tests were conducted under constant strain amplitude (0.01%), while the frequency was swept in the range of 0.1 to 60 Hz. The tests were performed under various magnitudes of applied magnetic flux densities ranging from -0.2 T to B=0.85 T in order to investigate the effect of both negative and positive magnetic field on the dynamic behavior of H-MREs. Moreover, a field-dependent phenomenological model has been proposed to predict the variation of storage and loss moduli of H-MREs under varying excitation frequency and applied magnetic flux density. The results show that the proposed model can accurately predict the viscoelastic behavior of H-MREs under various working conditions. Finally, a tunable vibration isolator based on H-MRE is developed and the transmissibility of the system is investigated. The results show that with lower and negative magnetic field and by less consuming energy, the vibration of payload could decrease remarkably in comparison with the positive magnetic field.

5.2 Contribution

The major contributions of this research to the advancement of characterization and modeling of hard magnetic particle based magnetorheological elastomers and developing a tunable vibration isolator based on H-MRE can be summarized as:

1. Dynamic characterization of magneto-mechanical properties of H-MRE sample under wide ranges of loading conditions and applied magnetic field intensities;

2. Formulation of a Phenomenological based mathematical model to predict the dynamic behavior of the MRE over wide ranges of loading frequencies and magnetic field intensities;

3. Developing a simple tunable vibration isolator based on H-MRE and investigating the effect of both positive and negative magnetic field on vibration isolation and transmissibility of the system;

5.3 Recommendations for future works

While the present research work has focused on characterization and modeling of hard magnetic particle based magnetorheological elastomers and developing a tunable vibration isolator based on H-MREs, there are still some future works which can be undertaken to evaluate the effect of different volume fraction of hard-particles on MR effect and development of a control strategy to examine the performance of vibration isolator based on H-MRE. Some potential future research studies are summarized as follows:

- Characterization of H-MREs with different volume fraction of hard-particles to better realize the effect of volume fraction on the viscoelastic properties and MR effect.
- Fabrication and characterization of anisotropic H-MREs under different ranges of loading conditions and applied magnetic field intensities in order to evaluate its behavior and its MR effect.
- While the proposed phenomenological models in this study agrees very well with the experimental results up to 30 Hz, there is a slight deviation between the developed

models and experimental results at higher frequencies. Thus, the developed models can be mainly used in the applications where the excitation frequency is mainly under 30 Hz such as seat suspension, vehicle suspension and some engine mounts. Considering this, developing phenomenological models that can accurately predict the experimental data beyond 30 Hz, would be helpful for design of H-MREs isolators operating at higher frequency ranges.

- Development of different semi-active control strategies to evaluate the real-time performance of H-MRE-based vibration isolators in suppressing vibration under varying harmonic and random excitations.

References

Agirre-Olabide I, Elejabarrieta MJ. (2016) Maximum attenuation variability of isotropic magnetosensitive elastomers. Polymer Testing. Sep 1;54:104-13.

Anderson K, Bravoco R, Hargrave W, Roche J, Von Lockette P and Lofland SE (2015) Dynamic shear response of hard versus soft magnetic magnetoactive elastomers. Smart Materials and Structures 24(2): 025022.

Asadi Khanouki M, Sedaghati R and Hemmatian M (2019) Experimental characterization and microscale modeling of isotropic and anisotropic magnetorheological elastomers. Composites Part B: Engineering 176: 107311.

Becker TI, Zimmermann K, Borin DY, Stepanov GV and Storozhenko PA (2018) Dynamic response of a sensor element made of magnetic hybrid elastomer with controllable properties. Journal of magnetism and magnetic materials 449: 77-82.

Bogdanov V, Borin D, Stepanov G and Andruszkiewicz A (2009) Usage of magneto-active elastomers in a bumper of a vehicle for front impact protection. Journal of Physics: Conference Series 149(1): 012089.

Borin DY, Stepanov GV and Odenbach S (2013) Tuning the tensile modulus of magnetorheological elastomers with magnetically hard powder. Journal of Physics: Conference Series 412(1): 012040.

Borin D, Stepanov G and Dohmen E (2019) Hybrid magnetoactive elastomer with a soft matrix and mixed powder. Archive of Applied Mechanics 89(1): 105-117.

Cantera MA, Behrooz M, Gibson RF, Gordaninejad F. Modeling of magneto-mechanical response of magnetorheological elastomers (MRE) and MRE-based systems: a review. Smart Materials and Structures. 2017 Jan 24;26(2):023001.

Carlson JD, Jolly MR. MR fluid, foam and elastomer devices. mechatronics. (2000) Jun 1;10(4-5):555-69.

Chen L, Gong XL, Jiang WQ, Yao JJ, Deng HX, Li WH. (2007) Investigation on magnetorheological elastomers based on natural rubber. Journal of Materials Science. Jul 1;42(14):5483-9.

Chen D, Song A, Hu X, Fu L and Ouyang Q (2019) A Spherical Actuator-Based Hand-Held Haptic Device for Touch Screen Interaction. IEEE Access 7:15125-15139.

Dargahi, A. (2017) Fabrication, Characterization and Modeling of Magnetorheological Elastomers, Concordia University.

Dargahi A, Sedaghati R, Rakheja S (2019) On the properties of magnetorheological elastomers in shear mode: Design, fabrication and characterization. Composites Part B: Engineering 159: 269-283.

Davis LC, (1999) Model of magnetorheological elastomers Journal of Applied Physics 85 3348

Deng HX, Gong XL and Wang LH (2006) Development of an adaptive tuned vibration absorber with magnetorheological elastomer. Smart Materials and Structures 15(5): N111–N116.

Deng, H. and Gong, X. (2008). Application of Magnetorheological Elastomer to vibration control. Communications in Nonlinear Science and Numerical Simulation. 13. 1938-1947. 10.1016/j.cnsns.2007.03.024.

Du G and Chen X (2012) MEMS magnetometer based on magnetorheological elastomer. Measurement, 45(1): 54-58.

Du H, Li W and Zhang N (2011) Semi-active variable stiffness vibration control of vehicle seat suspension using an MR elastomer isolator. Smart materials and structures 20(10): 105003.

Fan Lin, (2019) Design and Optimization of Magnetorheological Elastomer Based Adaptive Tuned Vibration Absorber, Concordia University.

Farshad M and Le Roux M (2004) A new active noise abatement barrier system. Polymer testing 23(7): 855-860.

Fletcher WP, Gent AN. (1954) Nonlinearity in the dynamic properties of vulcanized rubber compounds. Rubber Chemistry and Technology. Mar;27(1):209-22.

Ginder JM, Nichols ME, Elie LD and Tardiff, JL (1999) Magnetorheological elastomers: properties and applications. Proc. SPIE 3675, Smart Structures and Materials 1999: Smart Materials Technologies 3675: 131-138.

Ginder JM, Nichols ME, Elie LD and Clark SM (2000) Controllable-stiffness components based on magnetorheological elastomers. Proceedings of SPIE 3985: 418–425, doi:10.1117/12.388844.

Ginder JM, Schlotter WF and Nichols ME (2001) Magnetorheological elastomers in tunable vibration absorbers. Proceedings of SPIE 4331: 103–110, doi:10.1117/12.432694.

Gong XL, Zhang XZ, Zhang PQ. (2005) Fabrication and characterization of isotropic magnetorheological elastomers. Polymer testing. Aug 1;24(5):669-76.

Hitchcock GH, Gordaninejad F and Fuchs A (2006) Controllable magneto-rheological elastomer vibration isolator, US Patent 7086507.

Jolly MR, Carlson JD, Munoz BC. (1996) A model of the behaviour of magnetorheological materials. Smart Materials and Structures. 1996 Oct;5(5):607.

Jonsdottir F, Gudmundsson FB, Gudmundsson KH and Lecomte C (2015) Preparation and Characterization of a Prototype Magnetorheological Elastomer for Application in Prosthetic Devices. 7th ECCOMAS Thematic Conf. on Smart Structures and Materials.

Kallio M, Lindroos T, Aalto S, Jarvinen E, Karrna T, Meinander T (2007) Dynamic compression testing of a tunable spring element consisting of a magnetorheological elastomer Smart Materials and Structures 16 506-14

Kalina KA, Brummund J, Metsch P, Kästner M, Borin DY, Linke JM and Odenbach S (2017) Modeling of magnetic hystereses in soft MREs filled with NdFeB particles. Smart Materials and Structures 26(10): 105019.

Koo J H, Dawson A and Jung H J (2012) Characterization of actuation properties of magnetorheological elastomers with embedded hard magnetic particles. Journal of Intelligent Material Systems and Structures 23(9): 1049-1054.

Kramarenko EY, Chertovich AV, Stepanov GV, Semisalova AS, Makarova LA, Perov NS and Khokhlov AR (2015) Magnetic and viscoelastic response of elastomers with hard magnetic filler. Smart materials and structures 24(3): 035002.

Leblanc JL (2002) Rubber–filler interactions and rheological properties in filled compounds Progress in Polymer Science 27 627-87

Lee D, Lee M, Jung N, Yun M, Lee J, Thundat T and Jeon S (2014) Modulus-tunable magnetorheological elastomer microcantilevers. Smart Materials and Structures 23(5): 055017.

Lerner AA and Cunefare KA (2008) Performance of MRE based vibration absorbers. Journal of Intelligent Material Systems and Structures 19(5): 551–563.

Li Y, Li J, Tian T, Li W. (2013) A highly adjustable magnetorheological elastomer base isolator for applications of real-time adaptive control. Smart Materials and Structures. Aug 29;22(9):095020.

Li Y, Li J, Li W and Samali B (2013) Development and characterization of a magnetorheological elastomer based adaptive seismic isolator. Smart Materials and Structures 22(3): 035005.

Li, W., Zhang, X., and Du, H. (2013) Magnetorheological elastomers and their applications Advances in Elastomers I, pp. 357-374: Springer.

Li Y, Li J, Li W, Du H. A state-of-the-art review on magnetorheological elastomer devices. Smart materials and structures. 2014 Nov 12;23(12):123001.

Liao GJ, Gong XL, Xuan SH, Kang CJ, Zong LH. (2012) Development of a real-time tunable stiffness and damping vibration isolator based on magnetorheological elastomer. Journal of Intelligent Material Systems and Structures. Jan;23(1):25-33.

Liu YQ, Matsuhisa H and Utsuno H (2008) Semi-active vibration isolation system with variable stiffness and damping control. Journal of Sound and Vibration 313(1–2): 16–28.

Lokander, M., and Stenberg, B., (2003a) Performance of isotropic magnetorheological rubber materials Polymer Testing, vol. 22, no. 3, pp. 245-251.

Lokander M, Stenberg B. (2003b) Improving the magnetorheological effect in isotropic magnetorheological rubber materials. Polymer testing. Sep 1;22(6):677-80.

Lu X, Qiao X, Watanabe H, Gong X, Yang T, Li W, Sun K, Li M, Yang K, Xie H and Yin Q (2012) Mechanical and structural investigation of isotropic and anisotropic thermoplastic magnetorheological elastomer composites based on poly (styrene-b-ethylene-co-butylene-b-styrene)(SEBS). Rheologica acta 51(1): 37-50.

Megha S, Kumar S, D’Silva R. Vibration analysis of magnetorheological elastomer sandwich beam under different magnetic fields. International Journal of Vehicle Design (IJVD). 2016;6:75-80.

Ni ZC, Gong XL, Li JF and Chen L (2009) Study on a dynamic stiffness-tuning absorber with squeeze-strain enhanced magnetorheological elastomer. Journal of Intelligent Material Systems and Structures 20(10): 1195–1202.

Norouzi, M., Alehashem, S. M. S., Vatandoost, H., Ni, Y. Q., and Shahmardan, M. M. (2015) A new approach for modeling of magnetorheological elastomers Journal of Intelligent Material Systems and Structures.

Opie S and Yim W (2009) Design and control of a real-time variable stiffness vibration isolator. 2009 IEEE/ASME International Conference on Advanced Intelligent Mechatronics, Vols. 1–3, 380–385.

Payne AR, Whittaker RE (1971) Low Strain Dynamic Properties of Filled Rubbers *Rubber Chemistry and Technology* 44 440-78

Qian LJ, Xin FL, Bai XX and Wereley NM (2017) State observation–based control algorithm for dynamic vibration absorbing systems featuring magnetorheological elastomers: Principle and analysis. Journal of Intelligent Material Systems and Structures 28(18): 2539-2556.

Rendek M., and Lion A., (2010) Amplitude dependence of filler-reinforced rubber: Experiments, constitutive modelling and FEM – Implementation, International Journal of Solids and Structures, vol. 47, no. 21, pp. 2918-2936, 2010/10/15/.

Ruddy C, Ahearne E and Byrne G (2012) A review of magnetorheological elastomers: properties and applications. Advanced Manufacturing Science (AMS) Research. http://www. ucd. ie/mecheng/ams/news_items/Cillian% 20Ruddy. pdf Accessed 20.

Shen Y, Golnaraghi MF, Heppler GR (2004) Experimental Research and Modeling of Magnetorheological Elastomers Journal of Intelligent Material Systems and Structures 15 27-35

Sodeyama H, Suzuki K, Sunakoda K. Development of large capacity semi-active seismic damper using magneto-rheological fluid. J. Pressure Vessel Technol.. 2004 Feb 1;126(1):105-9.

Stepanov GV, Chertovich AV and Kramarenko EY (2012) Magnetorheological and deformation properties of magnetically controlled elastomers with hard magnetic filler. Journal of Magnetism and Magnetic Materials, 324(21): 3448-3451.

Stepanov GV, Borin DY, Kramarenko EY, Bogdanov VV, Semerenko DA and Storozhenko PA (2014) Magnetoactive elastomer based on magnetically hard filler: synthesis and study of viscoelastic and damping properties. Polymer science series A 56(5): 603-613.

Stepanov GV, Borin DY and Storozhenko PA (2017) Rotation of magnetic particles inside the polymer matrix of magnetoactive elastomers with a hard magnetic filler. Journal of Magnetism and Magnetic Materials 431: 138-140.

Stepanov GV, Borin DY, Bakhtiiarov AV and Storozhenko PA (2017) Magnetic properties of hybrid elastomers with magnetically hard fillers: rotation of particles. Smart Materials and Structures 26(3): 035060.

Sun SS, Yang J, Deng HX, Du H, Li WH, Alici G and Nakano M (2015) Horizontal vibration reduction of a seat suspension using negative changing stiffness magnetorheological elastomer isolators. International journal of vehicle design 68(1-3): 104-118.

Vatandoost, (2015), Fabrication and modeling of magnetorheological elastomer (MRE).

Vincent J, Staten, "Magnetic fluid clutch and brake," U.S. Patent 2,573,065, 1951.

Wang DH, Liao WH. (2005) Semiactive controllers for magnetorheological fluid dampers. Journal of intelligent material systems and structures. Dec;16(11-12):983-93.

Wang X, Gordaninejad F, Calgar M, Liu Y, Sutrisno J and Fuchs A (2009) Sensing behavior of magnetorheological elastomers. Journal of Mechanical Design 131(9).

Wen Q, Wang Y and Gong X (2017) The magnetic field dependent dynamic properties of magnetorheological elastomers based on hard magnetic particles. Smart Materials and Structures 26(7): 075012.

Woods BKS, Wereley N, Hoffmaster R, Nersessian N (2007) Manufacture of bulk magnetorheological elastomers using vacuum assisted resin transfer molding. International Journal of Modern Physics B. 21(28 and 29): 5010-5017.

Yang, J., Du, H., Li, W., Li, Y., Li, J., Sun, S., and Deng, H., (2013) Experimental study and modeling of a novel magnetorheological elastomer isolator Smart Materials and Structures, vol. 22, no. 11, pp. 117001.

Yang Z, Qin C, Rao Z, Ta N, Gong X. (2014) Design and analyses of axial semi-active dynamic vibration absorbers based on magnetorheological elastomers. Journal of Intelligent Material Systems and Structures. Nov;25(17):2199-207.

Yang J, Sun SS, Du H, Li WH, Alici G and Deng HX (2014) A novel magnetorheological elastomer isolator with negative changing stiffness for vibration reduction. Smart materials and structures 23(10): 105023.

Yoshioka H, Takahashi Y, Katayama K, Imazawa T, Murai N. (2001) An active microvibration isolation system for hi-tech manufacturing facilities. J. Vib. Acoust. Apr 1;123(2):269-75.

Ying ZG, Ni YQ and Ye SQ (2013) Stochastic micro-vibration suppression of a sandwich plate using a magneto-rheological visco-elastomer core. Smart materials and structures 23(2): 025019.

Yu, Y., Li, Y., Li, J., and Gu, X., (2016) A hysteresis model for dynamic behaviour of magnetorheological elastomer base isolator Smart Materials and Structures, vol. 25, no. 5, pp. 055029.

Zhou GY and Wang Q (2005) Magnetorheological elastomer-based smart sandwich beams with nonconductive skins. Smart Materials and Structures 14(5): 1001.

Zhao W, Pang H and Gong X (2017) Novel magnetorheological plastomer filled with NdFeB particles: preparation, characterization, and magnetic–mechanic coupling properties. Industrial & Engineering Chemistry Research 56(31): 8857-8863.